Nuclear Engineering and Technology 58 (2026) 103812

Contents lists available at ScienceDirect

Nuclear Engineering and Technology

journal homepage: www.elsevier.com/locate/net

Original Article

Computational analysis of propagation of geometrical uncertainties to tritium production in FNG WCLL experiment

Klemen Ambrožič [a,d,*], Gašper Žerovnik [a], Dieter Leichtle [b], Maurizio Angelone [c]

[a] Reactor Physics Department, Jožef Stefan Institute, Jamova cesta 39, Ljubljana, 1000, Slovenia
[b] Institute for Neutron Physics and Reactor Technology, Karlsruhe Institute of Technology, Hermann-von-Helmholtz-Platz 1, Eggenstein-Leopoldshafen, 76344, Germany
[c] Department of Fusion and Nuclear Safety Technology, Italian National Agency for New Technologies Energy and Sustainable Economic Development, Via E. Fermi, 45, Frascati-Rome, 00044, Italy
[d] Faculty of Mathematics and Physics, University of Ljubljana, Jadranska cesta 19, Ljubljana, 1000, Slovenia

ARTICLE INFO

MSC:
65C05
65C50
82D75
49K40

Keywords:
Geometrical uncertainties
Random sampling
Contributon field
Tritium breeding
Fusion

ABSTRACT

We present a computational sensitivity and uncertainty analysis of the effect of geometrical uncertainties on the measured reaction rates in the Water Cooled Lithium Lead experimental benchmark, which is a mock-up of a tritium breeding blanket for the future DEMO fusion facility. We used deterministic transport methods to determine the sensitivity of various parts of the geometry and Monte Carlo particle transport methods along with random sampling from geometrical uncertainties, to assess the expected uncertainty and sensitivity profiles, particularly to establish whether tritium self-sufficiency can be achieved within the uncertainty. We have established that most sensitive parts of the geometry are the source position and orientation, as well as the target detector pack position. We have established the uncertainty to be in the range of 8 % to 25 %, increasing with the distance from the source. We have also established the sensitivity to the displacement of the target detector pack to be roughly $5\,\%\,\mathrm{mm}^{-1}$, while the sensitivity to the perturbation of position of other detector packs and source position and orientation is generally below the $1\,\%\,\mathrm{mm}^{-1}$.

1. Introduction

The future fusion power plants are aiming at producing energy by fusing deuterium and tritium (D-T) fuel. Although deuterium is relatively abundant in nature (isotopic abundance of ≈0.0156 %), it is not the case for tritium (abundance of $< 1 \times 10^{-18}$) due to its short lifetime of 12.33 years, and will therefore have to be produced artificially by nuclear reactions. A dedicated breeding blanket (BB) component of the demonstration reactor DEMO will produce tritium via $^{6}\mathrm{Li}(n,T)\alpha$ and $^{7}\mathrm{Li}(n,nT)\alpha$ reactions, which will also act as a shield to the vacuum vessel, the superconducting magnets and other components from neutron radiation.

The breeding blanket needs to be designed to produce enough tritium, not only keep the reactor running (self-sufficiency), but also create a tritium surplus for starting up the plant, where losses due to tritium retention and radioactive decay have to be considered. The design and performance of the BB rely on neutron transport calculations, which have uncertainties stemming from modelling inaccuracies and nuclear data.

The Water Cooled Lithium Lead (WCLL) concept was recently selected for further testing in the International Thermonuclear Experimental Reactor (ITER) Test Blanket Module (TBM) [1] and is a promising candidate for Demonstration fusion power plant (DEMO) BB. A mock-up experiment of the WCLL blanket has been designed, constructed and irradiated at the Frascati D-T neutron generator (FNG).

The WCLL mock-up model consists of 110 LiPb bricks of $173\,\mathrm{mm} \times 90\,\mathrm{mm} \times 36\,\mathrm{mm}$ in size and 11 Eurofer-97 slabs with thickness of 9 mm. These bricks are arranged in blocks of $11 \times 5 \times 2$ bricks, with Eurofer-97 plates and water slabs in between representing structural elements and water cooling components, respectively.

In order to obtain experimental values for the tritium production rate (TPR), neutron activation of structural components and to measure various aspects of the neutron spectra, lithium TPR assessment detector packs along with pure Nb, Al, Ni, In and Au foil arrangements were embedded inside the LiPb centre blocks. The neutron detectors used in the mock-up can be divided into two groups of detector packs: TPR assessment dosimeter packets, consisting of lithium carbonate detectors (Li_2CO_3) with both natural and 95 % enriched in ^{6}Li. The second group

* Corresponding author at: Reactor Physics Department, Jožef Stefan Institute, Jamova cesta 39, Ljubljana, 1000, Slovenia.
E-mail address: klemen.ambrozic@ijs.si (K. Ambrožič).

https://doi.org/10.1016/j.net.2025.103812
Received 25 April 2025; Received in revised form 16 July 2025; Accepted 23 July 2025
Available online 29 August 2025

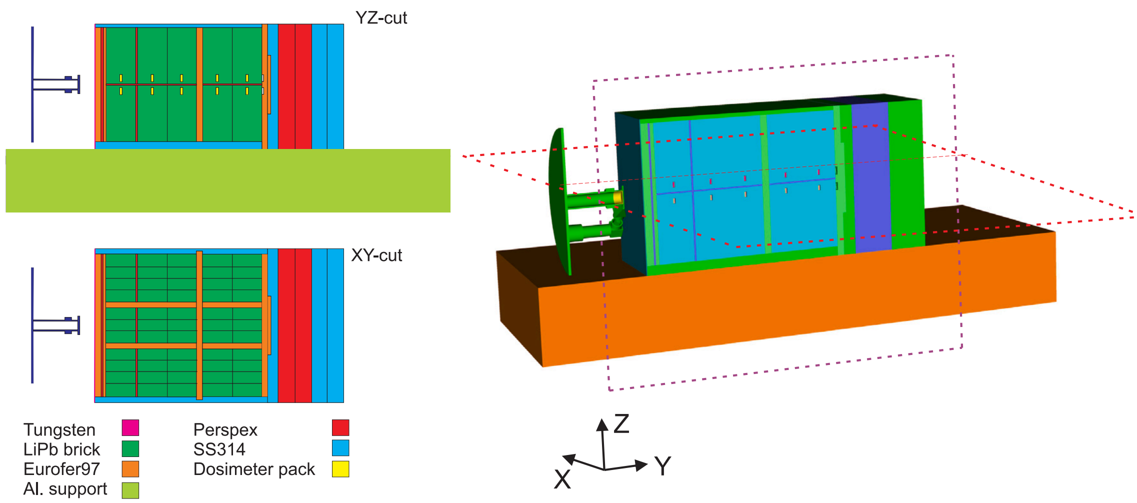

Fig. 1. WCLL computational model. Left: Schematics of the WCLL over the cut-planes with visible detector packs arranged in six columns and two rows. Right: 3D ray-traced cutout, with marked cut-planes.

of detector packs includes pure Nb, Al, Ni, In and Au foil arrangements for experimental determination of the characteristics of the neutron flux spectrum.

As mentioned, the mock-up consists of LiPb bricks stacked on top of each other, and the position uncertainty of the above-mentioned detector packs was estimated at $1\sigma = 1\,\mathrm{mm}$. The uncertainty in the position of the FNG neutron beam with respect to the WCLL's centre of was also considered as $1\sigma = 1\,\mathrm{mm}$. The directional misalignment of the neutron beam with respect to the front face of the WCLL assembly was considered in terms of the uncertainty in the direction vector by $1\sigma = 1\,\mathrm{mm}$, resulting in a mean angular divergence of 7.1° with maximum likelihood of 5.5°.

In order to assess the effects of these uncertainties and the sensitivity on the underlying reaction rates of individual detectors to these uncertainties, a two-fold analysis was performed. In the initial part of the analysis was performed by assessing the sensitivity of the model geometry to perturbations using deterministic calculations using the DENOVO code [2] for the forward and adjoint neutron flux and calculating the contribution field [3]. The second part was realized by performing a series of Monte Carlo particle transport simulations using the MCNP code [4], where above mentioned parameters of the model geometry were sampled from a normal distribution about the parameter's mean and its 1σ uncertainty. The analysis was performed by varying both the position of the detector pack and the misalignment and uncertainty of the directional vector of the neutron source beam with respect to the front face of the WCLL. Two distinct analyses were performed:

- Variation of a single uncertainty parameter per simulation i.e. one at a time.
- Variation of all of the uncertainty parameters per simulation i.e. all at once.

The neutron transport simulations were performed using three distinct nuclear data libraries: ENDF/B-VIII.0 [5], JEFF-3.3 [6] and FENDL-3.2b [7] in order to assess the effects of different cross section evaluations, primarily for the lithium-lead blocks, whose isotopic composition is shown in Table A.1. The dosimetric reaction rates were also tallied using multiple libraries: those mentioned above, as well as the dosimetric libraries IRDFF-II [8] and an older version, used in the initial reaction rate calculations IRDFF-v1.05 [9], where applicable.

The methods used in this work also open the possibilities of assessing the sensitivities of benchmark quality experiments and their quantities of interest to the input parameters and their uncertainties beforehand, to identify the highest contributing factors and impose more stringent requirements, improving the overall quality of such experiments.

2. Computational model

The base computational model used in our analysis is an MCNP model used in the initial analysis work [10], which was developed from the CAD model of the experimental mock-up for a pre-analysis of the WCLL mock-up device. The model, along with a validated FNG D-T fixed source description [11] were considered as a basis for our work. A picture of a 3D ray-traced MCNP model together with WCLL cut-out schematics are shown in Fig. 1. The top row of dosimeter packs contain Li_2CO_3 pellets with both natural Li content and 95 % enriched in ^{6}Li, to assess the TPR via $^6\mathrm{Li}(n,T)\alpha$ and $^7\mathrm{Li}(n,nT)\alpha$ reactions. The dosimeter packs in bottom row contain ^{93}Nb, ^{27}Al, $^{\mathrm{nat}}$Ni, In and Au dosimeters, in order to measure reaction rates for $^{93}\mathrm{Nb}(n,2n)^{92m}\mathrm{Nb}$, $^{27}\mathrm{Al}(n,\alpha)^{24}\mathrm{Na}$, $^{58}\mathrm{Ni}(n,2n)^{57}\mathrm{Ni}$, $^{58}\mathrm{Ni}(n,p)^{58}\mathrm{Co}$, $^{115}\mathrm{In}(n,n')^{115m}\mathrm{In}$, $^{197}\mathrm{Au}(n,2n)^{196}\mathrm{Au}$, $^{197}\mathrm{Au}(n,\gamma)^{198}\mathrm{Au}$ respectively. These reaction rates were measured in order to experimentally reconstruct the spectrum of incident neutrons via neutron spectrum unfolding [12] and to assess the neutron activation of structural materials in the proposed breeding blanket. These neutron dosimeters were also modelled in this work and their arrangement within their respective dosimeter packs is displayed in Fig. 2. The reaction cross sections for the above mentioned reactions from the IRDFF-II library are displayed in Fig. 3. A comparison of individual reaction cross sections and various nuclear data libraries in relation to those from IRDFF-II are displayed in Fig. B.12.

We have identified which parts of the geometry have the highest contribution intensities to individual reactions listed above, and are thus most susceptible to perturbations: the source and the dosimeters. Hence, we have performed a series of Monte Carlo particle transport calculations analysis, varying the positions and directions of individual dosimeter packs, as well as the position and orientation of the D-T neutron source with respect to the WCLL's front face.

3. Contributon analysis

The purpose of this analysis is to identify parts of the model geometry which affect the desired response function the most [3]. The

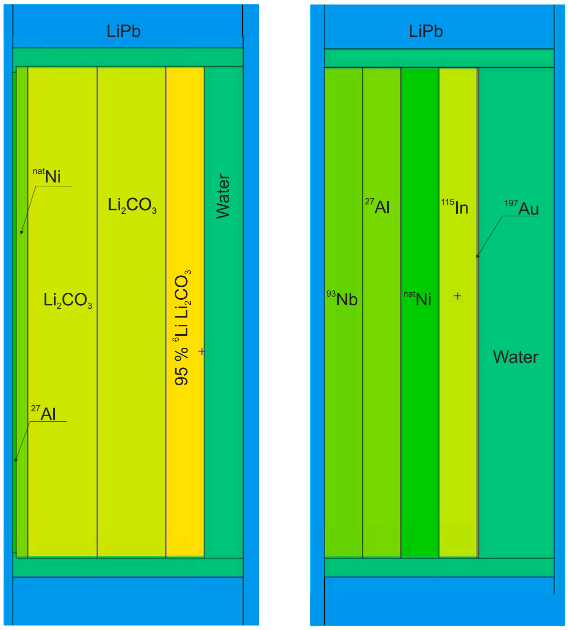

Fig. 2. Dosimeter arrangement within dosimeter packs. Top row dosimeter pack (z = 2 cm) for TPR assessment (left) and bottom row dosimeter pack (z = −2 cm) for assessment of various reaction rates (right).

calculations were performed using the DENOVO deterministic S_n neutron transport solver [2] within the ADVANTG package [13], which automatically converts the MCNP model and discretizes the geometry into a Cartesian mesh. In this case, it is very informative to calculate contribution field [3], defined by Eq. (1). By multiplying the forward and adjoint neutron flux (ϕ and $\phi^\dagger$ respectively), parts of the simulation phase space with the highest contribution field contribute the most to the response in the desired detector.

$$C = \phi \cdot \phi^\dagger \quad (1)$$

It can be noted that the computation of the contibuton field C requires solutions of both neutron flux ϕ and its adjoint $\phi^\dagger$. These solutions were obtained with the above mentioned codes, using 8 azimuthal and polar directions per octant for product quadrature (S8) set and 3rd order P_n expansion of the Legendre scattering angle. Multi-group neutron libraries with 27 energy groups [14] were based on the ENDF/B-VII.0 [15]. Reaction rate responses were modelled using a used defined response function, where the energy-dependent cross sections for the said reaction rates were taken from the IRDFF-II library [8]. The reader will note that particle transport libraries used here differ from the libraries used in the subsequent Monte Carlo particle transport analysis. This is due to the convenience, since they come as a standard library, and the aim is to assess the most sensitive parts of model geometry to perturbations.

As an example, Fig. 4 shows the case for the gold neutron dosimeter with two distinct contribution fields, corresponding to $^{197}\text{Au}(n,\gamma)$, susceptible to thermal neutrons, and $^{197}\text{Au}(n,2n)$, a fast neutron reaction. In both cases, the highest intensity of the contribution field is in close vicinity to the detector pack and the neutron source. In-between, the contribution field drops by one order of magnitude in case, where one is interested in the response of the detectors in the first column, to 2 to 3 orders of magnitude, when one is interested in the response of a detector in the last column. Similar contribution fields were observed for other reactions.

4. Random sampling of geometrical uncertainty

In this section, we describe the process, we have devised to assess the uncertainty and sensitivity to the perturbations to detector pack locations, as well as neutron source position and orientations with respect to the WCLL experiment front face.

The MCNP model was modified by replacing the coordinates of the detector packs, the D-T source location, the direction, and the associated geometry with unique placeholders. These were replaced with new coordinates randomly drawn from a normal distribution about the initial coordinate value and $1\sigma = 1\,\text{mm}$. Each of the newly constructed MCNP input files was also equipped with a unique random seed. The perturbations are schematically displayed in Fig. 5. Two distinct random sampling variants were performed:

- One-at-a-time: A single detector pack position or source position and orientation were perturbed at once, with the rest at nominal position, to assess the effect of an individual position/orientation perturbation. For the perturbation of each position/orientation, 512 MCNP input files were generated.
- All-at-once: Positions of all the detector packs, as well as the source positions and orientation were perturbed in each generated MCNP input file, 2048 in total.

Two sets of sensitivity profiles are obtained, adopting both all-at-once as well as one-at-a-time approach, and compared against each other. In order to assess the extent to which different nuclear data evaluations contribute to the uncertainty/sensitivity of the desired quantity, we have performed neutron transport calculations with three distinct nuclear data libraries: ENDF/B-VIII.0 [5], JEFF-3.3 [6] and FENDL-3.2b [7].

The analysis summary is made by merging multiple PDFs (Probability Density Function) of the reaction rate at the reference position (ref.) and the PDF due to varied geometry, arising from perturbing the source position and orientation, as well as perturbing the positions of all the detector packs (pert.). The PDFs are constructed by summation of Gaussian curves, mean values and standard deviations stemming from the mean and 1σ statistical uncertainties obtained by Monte Carlo particle transport, schematically displayed in Fig. 6. The uncertainties are similar to the uncertainties of unperturbed i.e. reference results. An example of the summary of the analysis results for All-at-once approach is shown in Figs. 7 and 8 for $^6\text{Li(n,T)}$ reaction on front Li_2CO_3 detector in the first and last column.

In case of perturbed samples, weighted histograms are also shown, where inverse squares of 1σ statistical uncertainties obtained from the Monte Carlo particle transport are used as weights. A limited set of results obtained using different nuclear data libraries for particle transport and IRDFF-II nuclear data libraries are displayed, while the analysis was performed for all the combinations. Unweighted and weighted statistics for perturbed samples i.e. mean and standard deviation are shown in Figs. 7 and 8, where one could note their deviation from maximum likelihood and associated confidence interval (1σ interval), pointing to non-central distribution, highlighting the benefit of using the total Monte Carlo approach compared to a deterministic analysis. A significant shift in the PDF's peak between the reference and perturbed samples is observed, which is exacerbated with the increasing distance from the source (increasing column number).

One can also observe a significant difference in PDFs due to different nuclear data libraries used for the particle transport. Although PDFs using ENDF/B-VIII.0 and FENDL-3.2b are a close match, they differ significantly from JEFF-3.3. The reaction rate uncertainty due to perturbations in case of $^6\text{Li(n,T)}$ reaction on front Li_2CO_3 detector range from 8 % in the detector packs in the first column, increasing to more than 25 % in the last column. The results of other reactions obtained by various combinations of nuclear data libraries used in particle transport and reaction rates are reported in Table C.2. The complete results and complementary graphs are reported in the Appendix C.

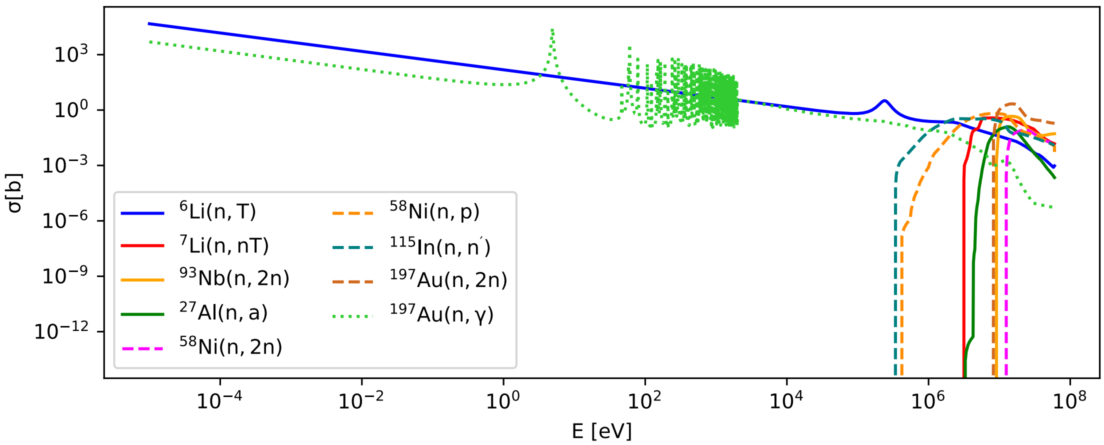

Fig. 3. Microscopic cross section vs. incident neutron energy for reactions of interest in the WCLL experiment from IRDFF-II nuclear data library.

In the bottom half of Fig. 9 one can note the point cloud displaying deviations of the detector pack from its reference position with colours signifying their respective reaction rates. The arrow signifies the linear sensitivity vector direction of the desired result, which is obtained by a least squares fit of the reaction rates to the position deviations. In general, an equation with number of linear terms corresponding to the number of degrees of freedom, plus a constant term were fitted to the data using the least-squares fit. Perturbing only the detector position results in a Fig. 9, where the point positions describe the deviation from the reference position in their respective directions, and the colour, denoting the reaction rate value, obtained from the Monte Carlo particle transport. One should note, that this is an illustrative case, considering only the movement of the detector pack. In general, one can limit itself only to the parts, most sensitive to perturbations, highlighted in the contribution field plots, resulting in 7 degrees of freedom: source movement and orientation, both in 2 axis, along with detector pack movement in 3 axis. When one considers all of the effect of other detector packs as well, the number increases to 34. Linear sensitivity/uncertainly coefficients from both All-at-once and One-at-a-time methods for ^{6}Li(n,T) on ^{nat}Li reaction rates on front Li_2CO_3 in detector pack at $z = 2\,\text{cm}$, columns 1 and 5, using the FENDL-3.2b nuclear data libraries for transport and IRDFF-II nuclear data libraries for reaction rates are reported in respectively, with the rest reported in supplementary materials.

The comparison of results obtained by All-at-once vs. One-at-a-time approach is displayed in Figs. 10 and 11. One can note that closest to the source (1st column), the perturbation of the position of the detector pack of interest has the largest effect on the resulting uncertainty and is comparable to the results obtained by the All-at-once approach. On the other hand, perturbation of other detector pack positions and the variation in source position and orientation has a smaller effect, but the maximum likelihood of their PDF is closer to the reference. This is also noticeable in the distribution of the point clouds, when comparing All-at-once and One-at-a-time approaches. In case when one is interested in reaction rates further away from the source, the effects between One-at-a-time and All-at-once approached appear virtually indistinguishable.

The effects of perturbing the position of the detector pack that holds the detector of interest are usually the highest, in the range of up to $5\,\%\,\text{mm}^{-1}$ of the displacement of the detector from the nominal position. The effects of source displacement and the uncertainly in its orientation are in the range of $1\,\%\,\text{mm}^{-1}$ or in terms of perturbation of the source direction. The sensitivity to position perturbations of other detector packs is usually below the $1\,\%\,\text{mm}^{-1}$ mark.

Although the All-at-once approach usually yields more information per computer time, it has some shortcomings. For this case in particular, the minimization algorithm was not able to infer a linear relationship between perturbations in the detector pack/source position and orientation for the dosimeter foils in the detector packs in the columns 4 and 5 for ^{58}Ni(n,2n) and ^{197}Au(n, α) and for aluminium dosimeter in the 5th column for ^{197}Au(n,2n) reaction, where only the maximum likelihood value was obtained. It does however take into account the correlations between individual effects. On the other hand, the One-at-a-time approach yielded sensitivity results for all detectors and reactions of interest independently.

Although the approach with random sampling of geometrical uncertainties described here yields superior results compared to deterministic transport methods, it is much more demanding in terms of computation resources. In this particular case, each particle transport simulation ran approximately 120 CPU-hours on a computer cluster, equipped with either Intel® Xeon® Gold 6148 or Intel® Xeon® Gold 6240R and 192 GB of memory. Although there are various perturbation techniques that allow the perturbation of various aspects of the computational model [16,17], they usually only capture linear or low-order dependence. Recent advances in porting Monte Carlo transport solvers to graphics processors (GPUs) such as OpenMC [18] and Shift code [19] shows 1 to 2 orders of magnitude increase in throughput, making such analysis much more convenient and affordable.

5. Conclusion

We present the computational analysis on the effects of the geometrical uncertainties to the measured reaction rates in the FNG WCLL mock-up experiment. The dimensional and position uncertainties are based on the expert assessment of the people performing the original experiment. The analysis was performed in two steps: initial determination of the geometry's sensitivity to the perturbation using the contribution field maps, calculated by the deterministic code DENOVO, which helped us with the identification of the most sensitive parts of the model geometry. In the second step, these perturbations were explicitly modelled and assessed using the Monte Carlo particle transport code MCNP for random sampling of geometric parameters. The perturbations were modelled by sampling from a normal distribution with its mean and standard deviation corresponding to the dimensional (or directional, in case of source orientation) nominal value and uncertainty respectively. We have used a generalized approach to identify the best estimate and the corresponding uncertainty of the quantity of interest, instead of relying on a simple mean and standard deviation estimates. Significant differences were observed between these two metrics, mainly due to the nonsymmetric PDFs. Two distinct approaches were used in our calculations: perturbing all of the parameters at once vs. perturbing one parameter at a time, in order to compare the performance of the two techniques. While all-at-once technique is generally more computationally efficient since it

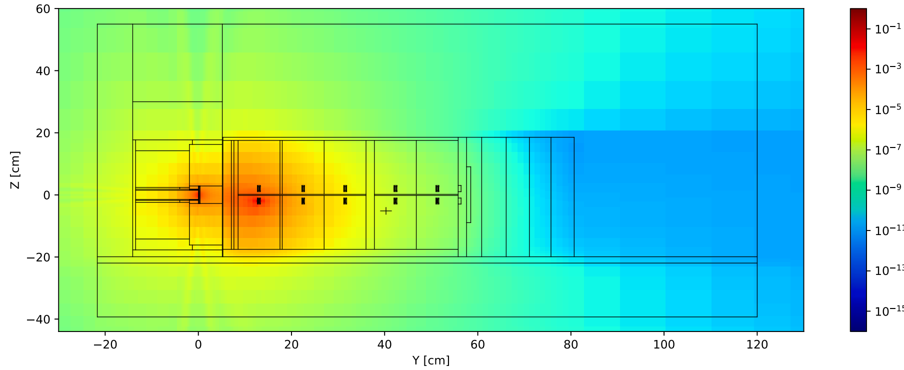

(4.a) ^{197}Au(n,γ), 1st column, bottom row.

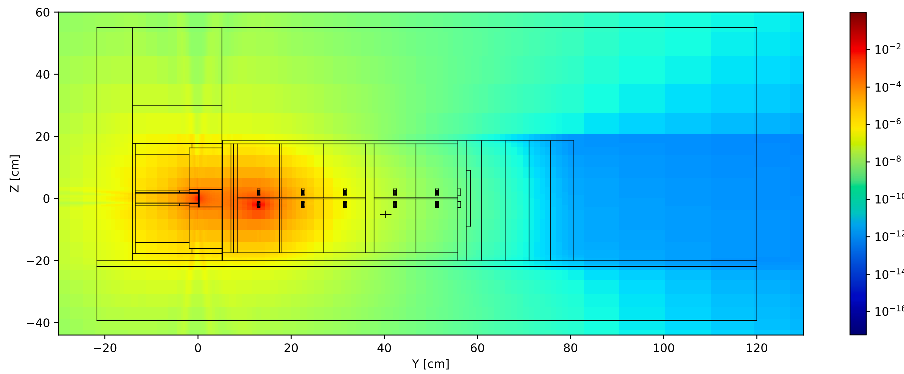

(4.b) ^{197}Au$(n,2n)$, 1st column, bottom row.

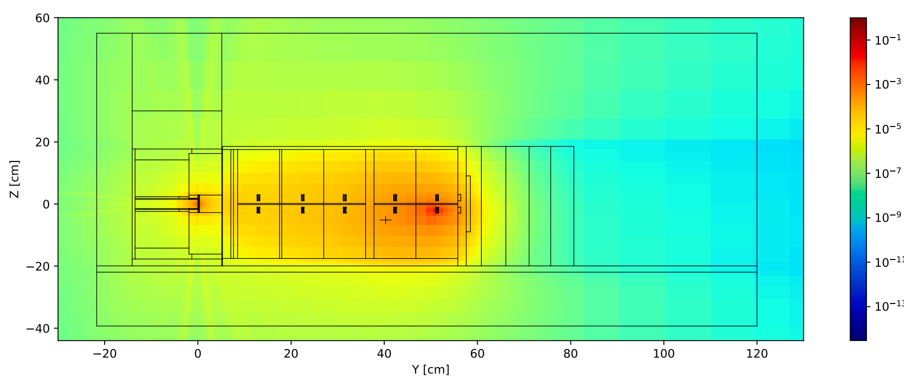

(4.c) ^{197}Au(n,γ), 5th column, bottom row.

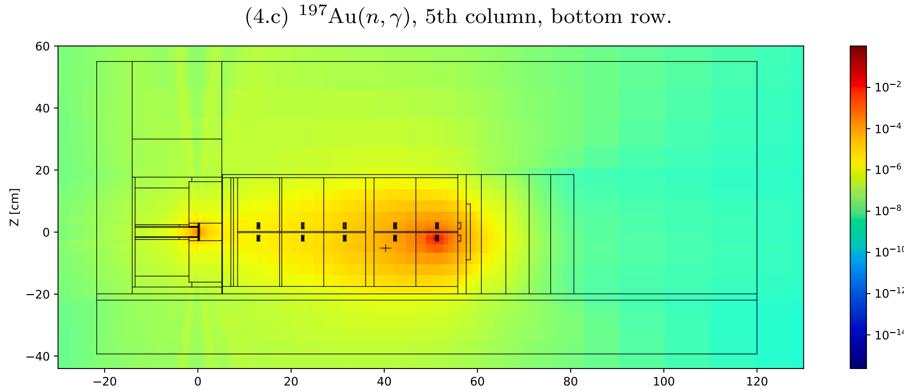

(4.d) ^{197}Au$(n,2n)$, 5th column, bottom row.

Fig. 4. Normalized contributon fields for ^{197}Au(n,γ) and ^{197}Au$(n,2n)$. The highest intensity can be observed near the source and detector.

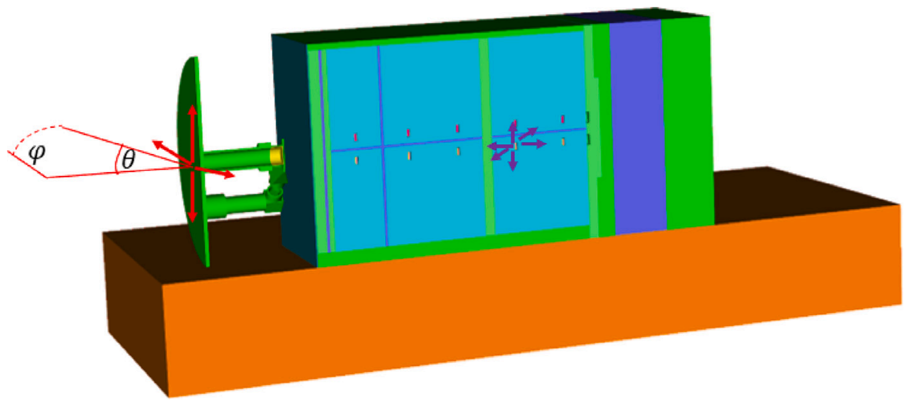

Fig. 5. Degrees of freedom for the position uncertainty of the detector package (purple) and source position and orientation (red) used in this work. (For interpretation of the references to colour in this figure legend, the reader is referred to the web version of this article.)

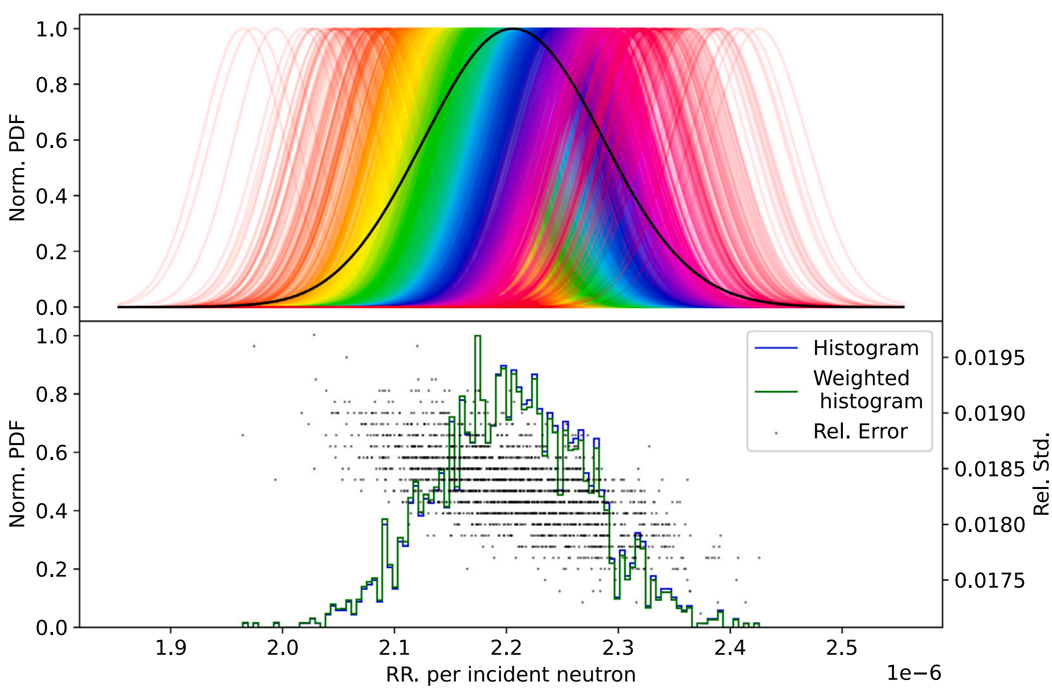

Fig. 6. Normally distributed results from individual MCNP evaluations (top, coloured) and resulting combined continuous distribution (top, black), as well as unweighted and weighted histograms, where uncertainty (relative terms shown on bottom plot) squares are taken as weights. Case for All-at-once approach, ^{93}Nb(n, 2n) on pure ^{93}Nb detector, bottom row, first column.

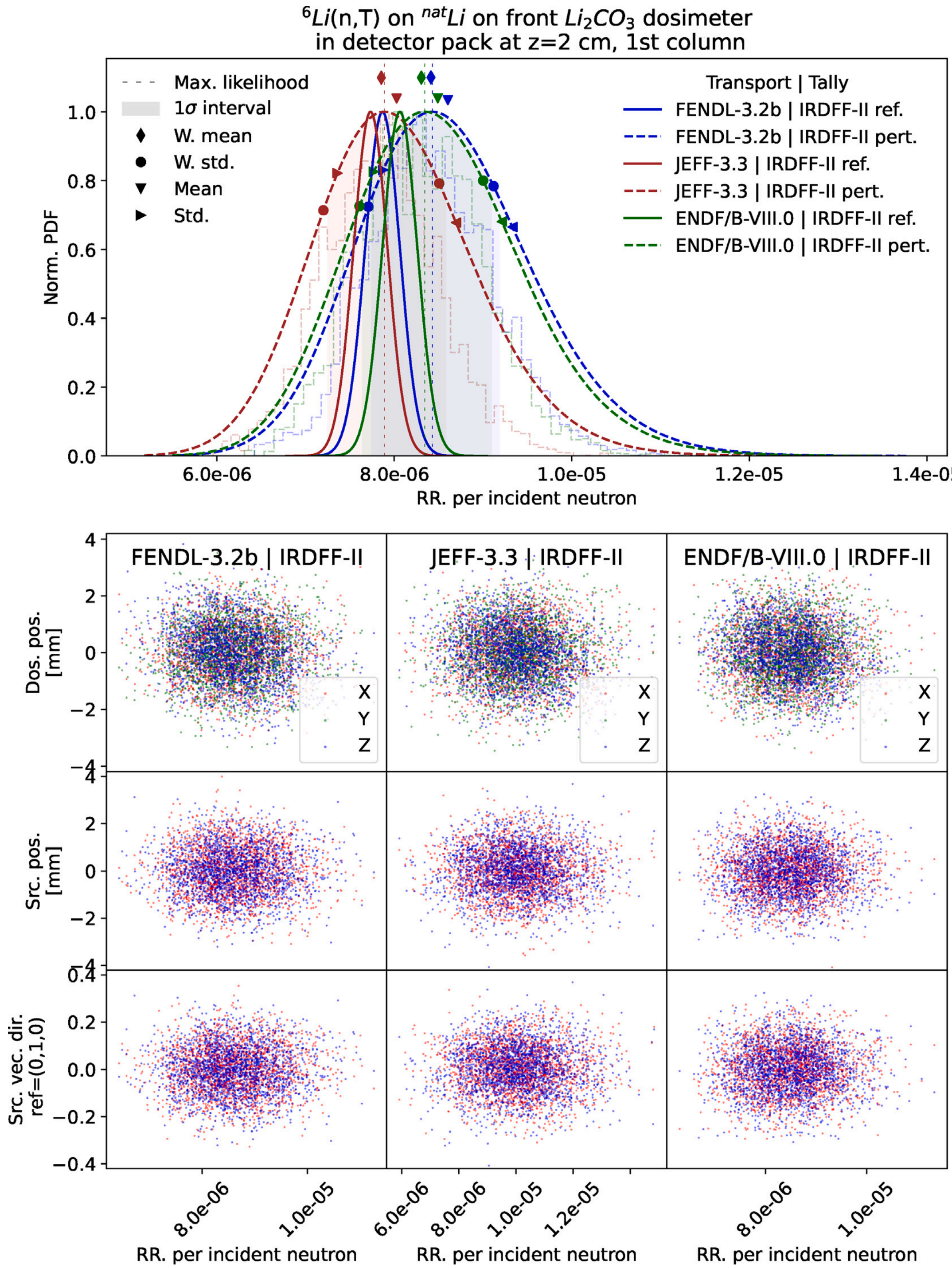

Fig. 7. ^{6}Li(n, T) on front Li_2CO_3 dosimeter, top row (z = 2 cm), 1st column with the point clouds below.

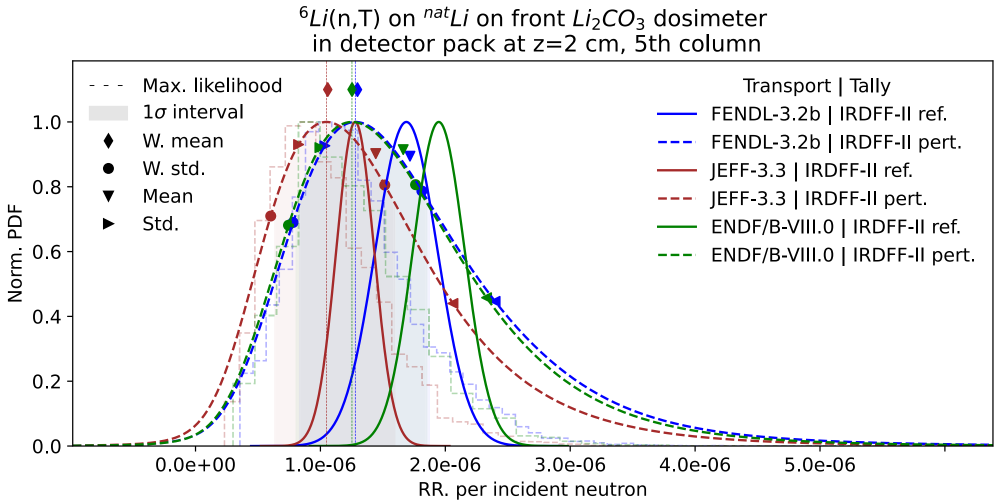

Fig. 8. ^{6}Li(n, T) on front Li_2CO_3 dosimeter, top row (z = 2 cm), 5th column.

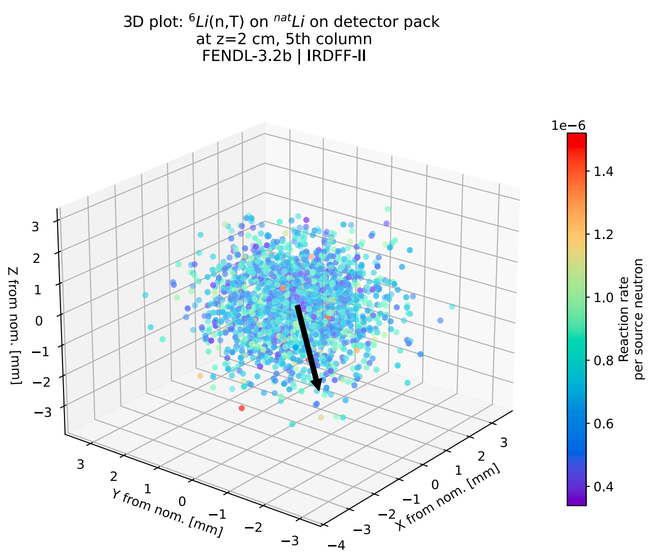

Fig. 9. Visualization of the sensitivity coefficient for the case of ^{6}Li(n, T) on front Li_2CO_3 detector, top row (z = 2 cm), 5th column.

provides information on the effects of all perturbations in a single run and can discern the correlation effects, it does not always capture the dependence even up to a linear term.

The methodology presented in this work shows promise in assessing the sensitivity to various input parameters such as uncertainties in geometry, material composition, nuclear data and others to minimize their effects on the desired observable beforehand so that high quality measurement data can be obtained from experimental benchmarks. We plan to use this methodology in the future, particularly for the assessment of concrete shielding performance in fusion devices using different concrete aggregate types, shape distributions and material compositions as well as the contents of impurities and water content.

Generally, this approach provides more data compared to deterministic sensitivity/uncertainty analysis, captures the non-symmetries of the resulting PDFs and provides a more accurate estimation of the best estimate and the uncertainty of the propagated dimensional or directional uncertainty. Although they are computationally very demanding, new techniques on parallelization of the Monte Carlo particle transport and deployment on GPUs promise to significantly increase the computational throughput, reducing the computational costs and make such analyses more affordable.

CRediT authorship contribution statement

Klemen Ambrožič: Writing – review & editing, Writing – original draft, Visualization, Software, Methodology, Investigation, Formal analysis, Data curation, Conceptualization. **Gašper Žerovnik:** Writing – review & editing, Supervision, Project administration, Conceptualization. **Dieter Leichtle:** Writing – review & editing, Supervision, Project administration, Funding acquisition. **Maurizio Angelone:** Writing – review & editing, Writing – original draft, Validation, Conceptualization.

Declaration of competing interest

The authors declare that they have no known competing financial interests or personal relationships that could have appeared to influence the work reported in this paper.

Acknowledgements

This work has been carried out within the framework of the EUROfusion Consortium, funded by the European Union via the Euratom Research and Training Programme (Grant Agreement No 101052200 — EUROfusion). Views and opinions expressed are however those of the author(s) only and do not necessarily reflect those of the European Union or the European Commission. Neither the European Union nor the European Commission can be held responsible for them.

Appendix A. LiPb material composition

See Table A.1.

Appendix B. Nuclear data comparison

Here we present the relevant neutron cross sections from different libraries, and compare them to the reference ones from IRDFF-II nuclear data library:

See Fig. B.12.

Appendix C. Analysis summary

See Tables C.2–C.4.

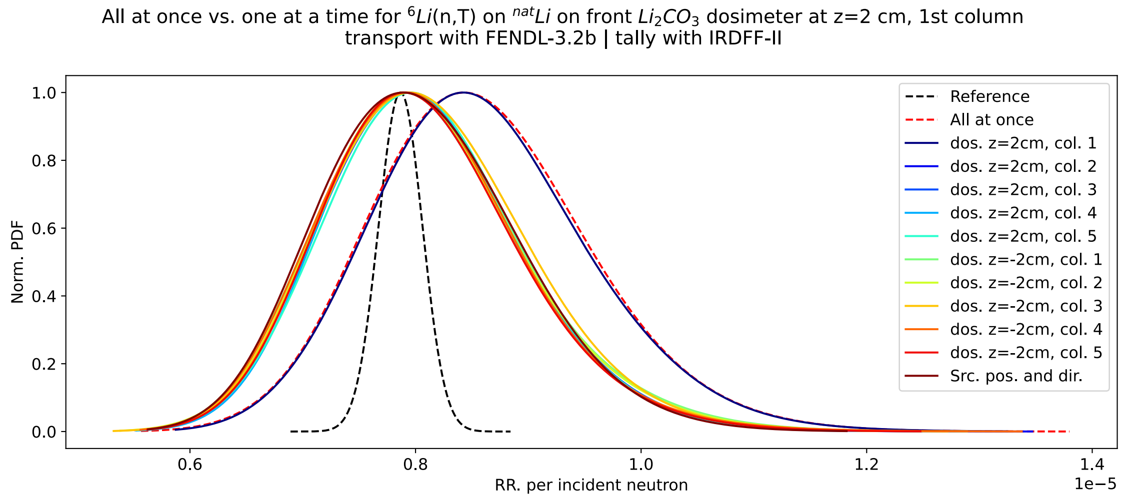

Fig. 10. Comparison on PDFs from One-at-a-time vs. All-at-once approaches for ^{6}Li(n, T) reactions rate on front Li_2CO_3 dosimeter, top row (z = 2 cm), 1st column.

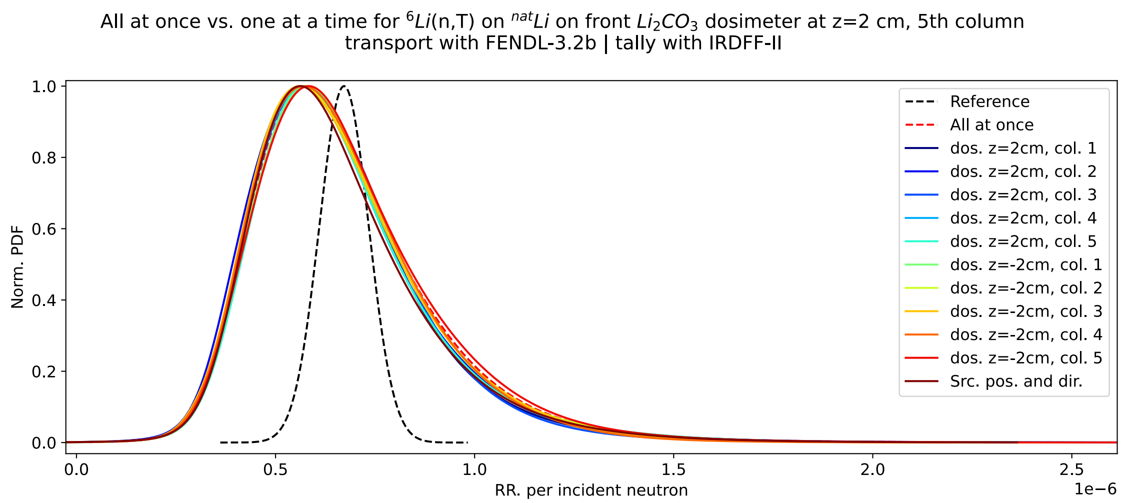

Fig. 11. Comparison on PDFs from One-at-a-time vs. All-at-once approaches for ^{6}Li(n, T) reactions rate on front Li_2CO_3 dosimeter, top row (z = 2 cm), 5th column.

Table A.1
Isotopic composition of the LiPb bricks — the main material of the WCLL benchmark experiment. Mass density $\rho = 10.48\ \mathrm{g\,cm^{-1}}$.

Nuclide	[b^{-1} cm^{-1}]	Nuclide	[b^{-1} cm^{-1}]	Nuclide	[b^{-1} cm^{-1}]
^{107}Ag	8.43492×10^{-6}	^{57}Fe	1.33198×10^{-6}	^{119}Sn	1.28310×10^{-6}
^{109}Ag	7.83645×10^{-6}	^{58}Fe	1.77261×10^{-7}	^{120}Sn	4.72952×10^{-6}
^{27}Al	6.50504×10^{-6}	^{55}Mn	3.19480×10^{-5}	^{122}Sn	6.85648×10^{-7}
^{74}As	1.17133×10^{-4}	^{95}Mo	2.90341×10^{-6}	^{124}Sn	8.57432×10^{-7}
^{209}Bi	1.67974×10^{-4}	^{93}Nb	1.88918×10^{-5}	^{130}Te	4.68762×10^{-6}
^{106}Cd	4.59274×10^{-9}	^{58}Ni	4.07153×10^{-5}	^{nat}V	6.89056×10^{-5}
^{108}Cd	3.24214×10^{-9}	^{60}Ni	1.56834×10^{-5}	^{182}W	2.52975×10^{-7}
^{110}Cd	4.54985×10^{-8}	^{61}Ni	6.81748×10^{-7}	^{183}W	1.36655×10^{-7}
^{111}Cd	4.70311×10^{-8}	^{62}Ni	2.17371×10^{-6}	^{184}W	2.92538×10^{-7}
^{112}Cd	8.86612×10^{-8}	^{64}Ni	5.53579×10^{-7}	^{186}W	2.71381×10^{-7}
^{113}Cd	4.45146×10^{-8}	^{106}Pd	4.50283×10^{-6}	^{64}Zn	1.30519×10^{-5}
^{114}Cd	1.04652×10^{-7}	^{121}Sb	8.24681×10^{-6}	^{66}Zn	7.48810×10^{-6}
^{116}Cd	2.75207×10^{-8}	^{28}Si	5.76322×10^{-6}	^{67}Zn	1.10040×10^{-6}
^{50}Cr	1.46669×10^{-6}	^{29}Si	2.93097×10^{-7}	^{68}Zn	5.03233×10^{-6}
^{52}Cr	2.82835×10^{-5}	^{30}Si	1.93107×10^{-7}	^{70}Zn	1.66402×10^{-7}
^{53}Cr	3.20715×10^{-6}	^{112}Sn	1.44890×10^{-7}	^{206}Pb	2.03446×10^{-1}
^{54}Cr	7.98323×10^{-7}	^{114}Sn	9.70913×10^{-8}	^{207}Pb	1.86562×10^{-1}
^{63}Cu	1.91051×10^{-5}	^{115}Sn	5.07863×10^{-8}	^{208}Pb	4.42349×10^{-1}
^{65}Cu	8.51540×10^{-6}	^{116}Sn	2.17187×10^{-6}	^{204}Pb	1.19208×10^{-2}
^{54}Fe	3.67410×10^{-6}	^{117}Sn	1.14717×10^{-6}	^{6}Li	5.36300×10^{-3}
^{56}Fe	5.76750×10^{-5}	^{118}Sn	3.61779×10^{-6}	^{7}Li	1.49637×10^{-1}

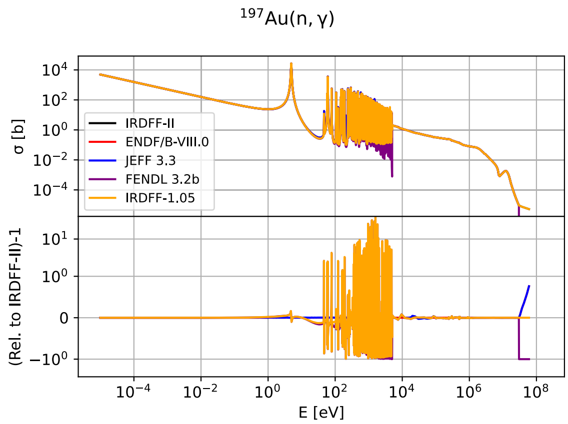

(B.12.a) ^{197}Au(n,γ) cross section data from various nuclear data libraries.

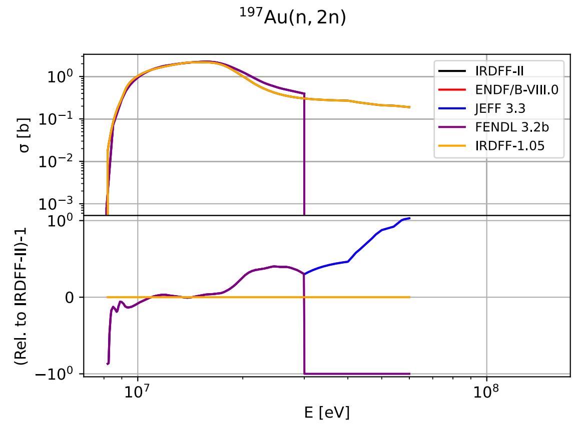

(B.12.b) ^{197}Au$(n,2n)$ cross section data from various nuclear data libraries.

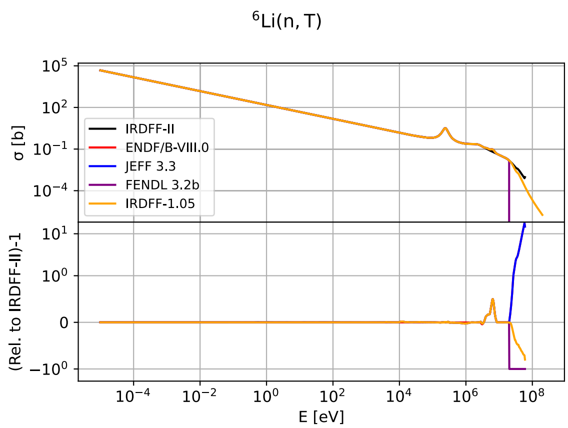

(B.12.c) ^{6}Li(n,T) cross section data from various nuclear data libraries.

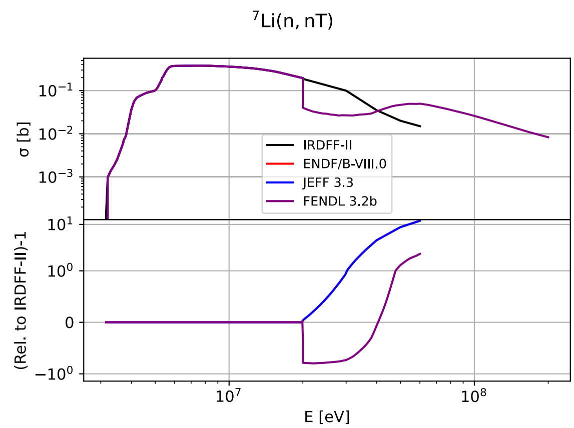

(B.12.d) ^{7}Li(n,nT) cross section data from various nuclear data libraries.

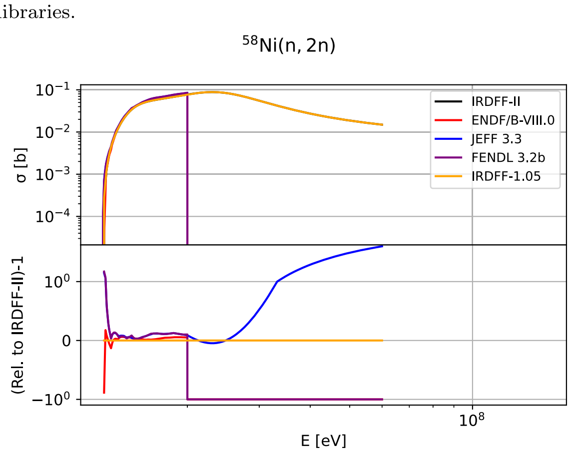

(B.12.e) ^{58}Ni$(n,2n)$ cross section data from various nuclear data libraries.

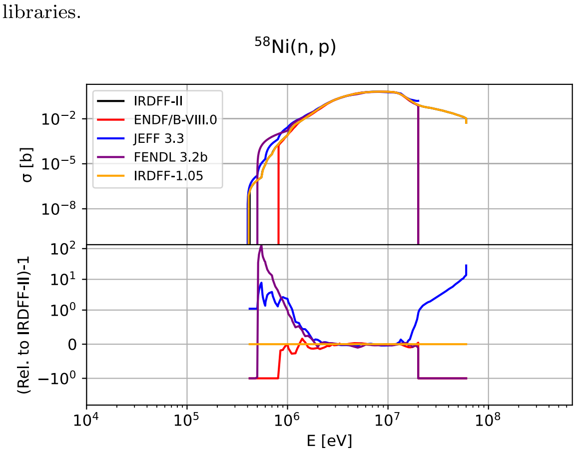

(B.12.f) ^{58}Ni(n,p) cross section data from various nuclear data libraries.

Fig. B.12. Neutron reaction cross sections, taken from various nuclear data libraries, and compared to IRDFF-II. The y axis on comparison graphs has linear scale between $(-1,1)$ and logarithmic otherwise.

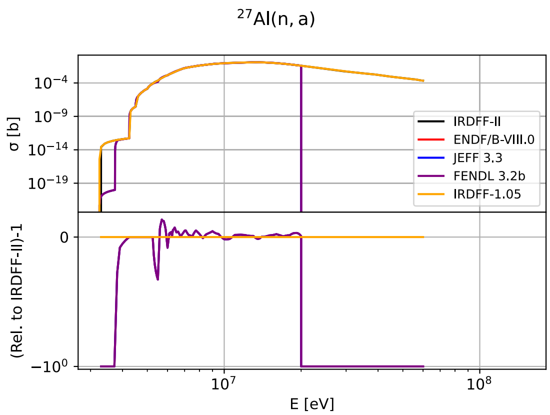

(B.12.g) $^{27}\mathrm{Al}(n,a)$ cross section data from various nuclear data libraries.

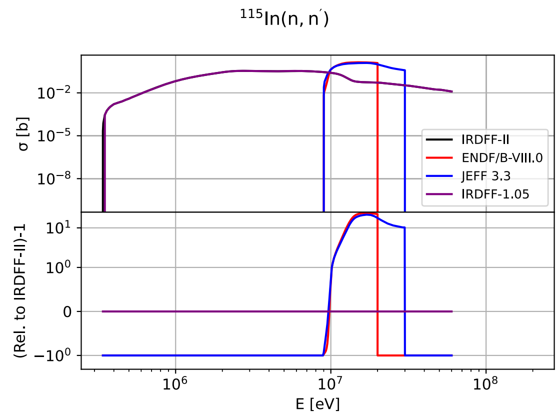

(B.12.h) $^{115}\mathrm{In}(n,n')$ cross section data from various nuclear data libraries.

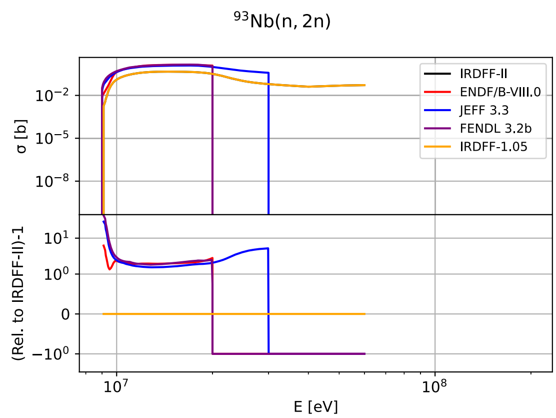

(B.12.i) $^{93}\mathrm{Nb}(n,2n)$ cross section data from various nuclear data libraries.

Fig. B.12. (*continued*).

Table C.2
Displaying reaction rates per atom per source neutron, their best estimates and uncertainties using different metrics (unweighted vs. weighted) of the reference calculation (Ref.), perturbing the uncertainties all at once (All at once) and only the dosimeter pack position (One at a time) using FENDL-3.2b nuclear data library for neutron transport and IRDFF-II nuclear data library for reaction rate tallying.

Quantity	Position	Dosimeter	Method	FENDL-3.2b						
				Mean	Std.	W. Mean	W. Std	Max. Likelihood	1σ min. bound	1σ max. bound
		front Li_2CO_3	Ref.	1.29e-03	3.41e-06	1.29e-03	3.41e-06	1.29e-03	1.28e-03	1.29e-03
			All at once	1.35e-03	3.75e-05	1.35e-03	3.79e-05	1.37e-03	1.28e-03	1.41e-03
			One at a time	1.35e-03	3.92e-05	1.35e-03	3.98e-05	1.37e-03	1.27e-03	1.41e-03
	z=2 cm,1st column	back Li_2CO_3	Ref.	1.21e-03	3.38e-06	1.21e-03	3.38e-06	1.21e-03	1.20e-03	1.21e-03
			All at once	1.30e-03	4.82e-05	1.29e-03	4.88e-05	1.31e-03	1.19e-03	1.37e-03
			One at a time	1.29e-03	4.97e-05	1.29e-03	5.03e-05	1.32e-03	1.19e-03	1.37e-03
		enriched Li_2CO_3	Ref.	1.19e-03	3.62e-06	1.19e-03	3.62e-06	1.19e-03	1.19e-03	1.20e-03
			All at once	1.28e-03	4.85e-05	1.27e-03	4.91e-05	1.29e-03	1.25e-03	1.33e-03
			One at a time	1.27e-03	4.95e-05	1.27e-03	5.01e-05	1.29e-03	1.26e-03	1.33e-03
		front Li_2CO_3	Ref.	5.51e-04	2.29e-06	5.51e-04	2.29e-06	5.51e-04	5.49e-04	5.53e-04
			All at once	5.67e-04	2.16e-05	5.66e-04	2.14e-05	5.52e-04	5.41e-04	5.66e-04
			One at a time	5.67e-04	2.24e-05	5.66e-04	2.23e-05	5.52e-04	5.40e-04	5.70e-04
	z=2 cm,2nd column	back Li_2CO_3	Ref.	5.17e-04	2.23e-06	5.17e-04	2.23e-06	5.17e-04	5.15e-04	5.19e-04
			All at once	5.37e-04	2.67e-05	5.36e-04	2.64e-05	5.19e-04	4.95e-04	5.88e-04
			One at a time	5.39e-04	2.76e-05	5.37e-04	2.75e-05	5.19e-04	5.07e-04	5.31e-04
		enriched Li_2CO_3	Ref.	5.08e-04	2.42e-06	5.08e-04	2.42e-06	5.08e-04	5.05e-04	5.10e-04
			All at once	5.29e-04	2.64e-05	5.27e-04	2.62e-05	5.11e-04	4.86e-04	5.80e-04
			One at a time	5.30e-04	2.76e-05	5.29e-04	2.74e-05	5.10e-04	4.98e-04	5.24e-04
		front Li_2CO_3	Ref.	2.65e-04	1.61e-06	2.65e-04	1.61e-06	2.65e-04	2.63e-04	2.67e-04
Total flux			All at once	2.71e-04	1.14e-05	2.71e-04	1.13e-05	2.67e-04	2.59e-04	2.80e-04
			One at a time	2.73e-04	1.17e-05	2.73e-04	1.17e-05	2.69e-04	2.59e-04	2.84e-04
	z=2 cm,3rd column	back Li_2CO_3	Ref.	2.48e-04	1.56e-06	2.48e-04	1.56e-06	2.48e-04	2.47e-04	2.50e-04

(*continued on next page*)

Table C.2 (*continued*).

			All at once	2.57e-04	1.35e-05	2.57e-04	1.34e-05	2.49e-04	2.41e-04	2.60e-04
			One at a time	2.59e-04	1.44e-05	2.59e-04	1.43e-05	2.50e-04	2.42e-04	2.63e-04
		enriched Li_2CO_3	Ref.	2.44e-04	1.68e-06	2.44e-04	1.68e-06	2.44e-04	2.42e-04	2.45e-04
			All at once	2.54e-04	1.37e-05	2.53e-04	1.36e-05	2.47e-04	2.38e-04	2.59e-04
			One at a time	2.56e-04	1.44e-05	2.55e-04	1.43e-05	2.48e-04	2.38e-04	2.65e-04
	z=2 cm,4th column	front Li_2CO_3	Ref.	1.15e-04	1.06e-06	1.15e-04	1.06e-06	1.15e-04	1.14e-04	1.16e-04
			All at once	1.16e-04	5.33e-06	1.16e-04	5.29e-06	1.15e-04	1.10e-04	1.20e-04
			One at a time	1.16e-04	5.28e-06	1.15e-04	5.26e-06	1.15e-04	1.10e-04	1.20e-04
		back Li_2CO_3	Ref.	1.13e-04	1.04e-06	1.13e-04	1.04e-06	1.13e-04	1.12e-04	1.14e-04
			All at once	1.12e-04	6.21e-06	1.12e-04	6.15e-06	1.11e-04	1.05e-04	1.17e-04
			One at a time	1.11e-04	6.06e-06	1.11e-04	6.05e-06	1.11e-04	1.06e-04	1.16e-04
		enriched Li_2CO_3	Ref.	1.13e-04	1.14e-06	1.13e-04	1.14e-06	1.13e-04	1.12e-04	1.14e-04
			All at once	1.10e-04	6.46e-06	1.10e-04	6.40e-06	1.09e-04	1.03e-04	1.15e-04
			One at a time	1.10e-04	6.47e-06	1.09e-04	6.42e-06	1.09e-04	1.03e-04	1.15e-04
	z=2 cm,5th column	front Li_2CO_3	Ref.	5.42e-05	7.26e-07	5.42e-05	7.26e-07	5.42e-05	5.35e-05	5.49e-05
			All at once	5.42e-05	3.38e-06	5.39e-05	3.37e-06	5.38e-05	5.05e-05	5.73e-05
			One at a time	5.43e-05	3.30e-06	5.40e-05	3.28e-06	5.37e-05	5.05e-05	5.72e-05
		back Li_2CO_3	Ref.	5.16e-05	6.96e-07	5.16e-05	6.96e-07	5.16e-05	5.09e-05	5.23e-05
			All at once	5.21e-05	3.62e-06	5.18e-05	3.59e-06	5.15e-05	4.81e-05	5.52e-05
			One at a time	5.25e-05	3.51e-06	5.22e-05	3.50e-06	5.20e-05	4.86e-05	5.55e-05
		enriched Li_2CO_3	Ref.	5.06e-05	7.54e-07	5.06e-05	7.54e-07	5.06e-05	4.98e-05	5.13e-05
			All at once	5.11e-05	3.75e-06	5.07e-05	3.72e-06	5.05e-05	4.69e-05	5.44e-05
			One at a time	5.14e-05	3.70e-06	5.10e-05	3.69e-06	5.08e-05	4.73e-05	5.46e-05
^{6}Li(n,T) on ^{nat}Li	z=2 cm,1st column	front Li_2CO_3	Ref.	7.87e-06	1.48e-07	7.87e-06	1.48e-07	7.87e-06	7.72e-06	8.01e-06
			All at once	8.60e-06	7.28e-07	8.41e-06	7.05e-07	8.43e-06	7.75e-06	9.18e-06
			One at a time	8.60e-06	7.18e-07	8.42e-06	6.93e-07	8.42e-06	7.77e-06	9.14e-06
		back Li_2CO_3	Ref.	7.05e-06	1.31e-07	7.05e-06	1.31e-07	7.05e-06	6.92e-06	7.18e-06
			All at once	7.68e-06	6.60e-07	7.51e-06	6.41e-07	7.54e-06	6.94e-06	8.20e-06
			One at a time	7.70e-06	6.80e-07	7.52e-06	6.64e-07	7.55e-06	6.94e-06	8.22e-06
	z=2 cm,2nd column	front Li_2CO_3	Ref.	6.35e-06	1.35e-07	6.35e-06	1.35e-07	6.35e-06	6.22e-06	6.49e-06
			All at once	6.54e-06	6.72e-07	6.35e-06	6.53e-07	6.35e-06	5.74e-06	7.05e-06
			One at a time	6.56e-06	6.59e-07	6.37e-06	6.42e-07	6.36e-06	5.73e-06	7.08e-06
		back Li_2CO_3	Ref.	5.22e-06	1.12e-07	5.22e-06	1.12e-07	5.22e-06	5.11e-06	5.34e-06
			All at once	5.60e-06	6.10e-07	5.41e-06	5.83e-07	5.40e-06	4.86e-06	6.02e-06
			One at a time	5.59e-06	5.67e-07	5.45e-06	5.52e-07	5.46e-06	4.92e-06	6.04e-06
	z=2 cm,3rd column	front Li_2CO_3	Ref.	2.58e-06	6.95e-08	2.58e-06	6.95e-08	2.58e-06	2.51e-06	2.65e-06
			All at once	2.75e-06	3.62e-07	2.60e-06	3.29e-07	2.61e-06	2.30e-06	2.97e-06
			One at a time	2.77e-06	3.52e-07	2.63e-06	3.27e-07	2.64e-06	2.33e-06	2.99e-06
		back Li_2CO_3	Ref.	2.28e-06	6.64e-08	2.28e-06	6.64e-08	2.28e-06	2.21e-06	2.34e-06
			All at once	2.42e-06	3.23e-07	2.28e-06	2.93e-07	2.28e-06	2.01e-06	2.60e-06
			One at a time	2.46e-06	3.27e-07	2.33e-06	3.06e-07	2.33e-06	2.05e-06	2.67e-06
	z=2 cm,4th column	front Li_2CO_3	Ref.	1.08e-06	4.95e-08	1.08e-06	4.95e-08	1.08e-06	1.03e-06	1.13e-06
			All at once	1.17e-06	2.14e-07	1.06e-06	1.78e-07	1.06e-06	8.98e-07	1.26e-06
			One at a time	1.16e-06	2.13e-07	1.06e-06	1.69e-07	1.06e-06	8.92e-07	1.25e-06
		back Li_2CO_3	Ref.	1.03e-06	5.53e-08	1.03e-06	5.53e-08	1.03e-06	9.71e-07	1.08e-06
			All at once	1.06e-06	1.96e-07	9.59e-07	1.61e-07	9.60e-07	8.12e-07	1.14e-06
			One at a time	1.06e-06	1.94e-07	9.62e-07	1.52e-07	9.50e-07	8.16e-07	1.12e-06
	z=2 cm,5th column	front Li_2CO_3	Ref.	6.72e-07	4.71e-08	6.72e-07	4.71e-08	6.72e-07	6.25e-07	7.19e-07
			All at once	6.79e-07	1.70e-07	5.74e-07	1.29e-07	5.70e-07	4.59e-07	7.18e-07
			One at a time	6.77e-07	1.70e-07	5.76e-07	1.24e-07	5.71e-07	4.65e-07	7.11e-07
		back Li_2CO_3	Ref.	5.50e-07	2.84e-08	5.50e-07	2.84e-08	5.50e-07	5.22e-07	5.78e-07
			All at once	6.09e-07	1.48e-07	5.20e-07	1.14e-07	5.21e-07	4.19e-07	6.53e-07
			One at a time	6.19e-07	1.53e-07	5.34e-07	1.13e-07	5.40e-07	4.36e-07	6.65e-07
^{7}Li(n,XT) on ^{nat}Li	z=2 cm,1st column	front Li_2CO_3	Ref.	2.18e-06	9.55e-09	2.18e-06	9.55e-09	2.18e-06	2.17e-06	2.19e-06
			All at once	2.20e-06	6.61e-08	2.20e-06	6.60e-08	2.20e-06	2.14e-06	2.26e-06
			One at a time	2.20e-06	6.30e-08	2.20e-06	6.30e-08	2.20e-06	2.14e-06	2.26e-06
		back Li_2CO_3	Ref.	2.05e-06	9.33e-09	2.05e-06	9.33e-09	2.05e-06	2.04e-06	2.06e-06
			All at once	2.09e-06	7.46e-08	2.09e-06	7.44e-08	2.09e-06	2.02e-06	2.16e-06
			One at a time	2.10e-06	7.32e-08	2.09e-06	7.32e-08	2.09e-06	2.02e-06	2.16e-06
	z=2 cm,2nd column	front Li_2CO_3	Ref.	3.76e-07	4.07e-09	3.76e-07	4.07e-09	3.76e-07	3.72e-07	3.80e-07
			All at once	3.77e-07	1.84e-08	3.75e-07	1.84e-08	3.76e-07	3.57e-07	3.95e-07
			One at a time	3.77e-07	1.95e-08	3.76e-07	1.95e-08	3.75e-07	3.57e-07	3.95e-07
		back Li_2CO_3	Ref.	3.52e-07	3.94e-09	3.52e-07	3.94e-09	3.52e-07	3.48e-07	3.56e-07
			All at once	3.56e-07	1.94e-08	3.54e-07	1.93e-08	3.53e-07	3.34e-07	3.73e-07
			One at a time	3.57e-07	2.02e-08	3.55e-07	2.02e-08	3.54e-07	3.34e-07	3.75e-07
	z=2 cm,3rd column	front Li_2CO_3	Ref.	8.77e-08	1.93e-09	8.77e-08	1.93e-09	8.77e-08	8.58e-08	8.97e-08
			All at once	9.36e-08	8.68e-09	9.24e-08	8.61e-09	9.24e-08	8.34e-08	1.02e-07
			One at a time	9.36e-08	8.82e-09	9.24e-08	8.74e-09	9.24e-08	8.33e-08	1.02e-07

(continued on next page)

Table C.2 (*continued*).

		back Li_2CO_3	Ref.	8.18e-08	1.88e-09	8.18e-08	1.88e-09	8.18e-08	7.99e-08	8.36e-08
			All at once	8.81e-08	8.89e-09	8.68e-08	8.78e-09	8.66e-08	7.79e-08	9.60e-08
			One at a time	8.85e-08	9.09e-09	8.72e-08	9.02e-09	8.73e-08	7.81e-08	9.68e-08
	z=2 cm,4th column	front Li_2CO_3	Ref.	2.03e-08	9.45e-10	2.03e-08	9.45e-10	2.03e-08	1.93e-08	2.12e-08
			All at once	1.95e-08	4.13e-09	1.83e-08	3.93e-09	1.82e-08	1.43e-08	2.26e-08
			One at a time	1.92e-08	3.89e-09	1.80e-08	4.01e-09	1.86e-08	1.45e-08	2.30e-08
		back Li_2CO_3	Ref.	1.99e-08	9.48e-10	1.99e-08	9.48e-10	1.99e-08	1.90e-08	2.09e-08
			All at once	1.87e-08	3.97e-09	1.74e-08	3.91e-09	1.76e-08	1.37e-08	2.19e-08
			One at a time	1.85e-08	4.01e-09	1.72e-08	4.00e-09	1.77e-08	1.37e-08	2.19e-08
	z=2 cm,5th column	front Li_2CO_3	Ref.	6.22e-09	5.99e-10	6.22e-09	5.99e-10	6.22e-09	5.62e-09	6.82e-09
			All at once	5.97e-09	2.18e-09	4.82e-09	2.08e-09	4.95e-09	3.02e-09	7.26e-09
			One at a time	5.97e-09	2.17e-09	4.76e-09	2.12e-09	4.98e-09	3.15e-09	7.21e-09
		back Li_2CO_3	Ref.	5.91e-09	5.81e-10	5.91e-09	5.81e-10	5.91e-09	5.33e-09	6.49e-09
			All at once	5.77e-09	2.22e-09	4.51e-09	2.09e-09	4.68e-09	2.80e-09	6.94e-09
			One at a time	5.67e-09	2.14e-09	4.37e-09	2.12e-09	4.77e-09	2.94e-09	6.92e-09
^{6}Li(n,T) on 95% ^{6}Li	z=2 cm,1st column	enriched Li_2CO_3	Ref.	7.71e-05	1.10e-06	7.71e-05	1.10e-06	7.71e-05	7.60e-05	7.82e-05
			All at once	8.32e-05	5.67e-06	8.23e-05	5.69e-06	8.29e-05	7.74e-05	8.85e-05
			One at a time	8.31e-05	5.35e-06	8.23e-05	5.39e-06	8.27e-05	7.72e-05	8.83e-05
	z=2 cm,2nd column	enriched Li_2CO_3	Ref.	5.40e-05	9.69e-07	5.40e-05	9.69e-07	5.40e-05	5.30e-05	5.49e-05
			All at once	5.52e-05	4.81e-06	5.43e-05	4.76e-06	5.43e-05	4.97e-05	5.91e-05
			One at a time	5.53e-05	4.74e-06	5.44e-05	4.66e-06	5.44e-05	4.96e-05	5.95e-05
	z=2 cm,3rd column	enriched Li_2CO_3	Ref.	2.49e-05	6.08e-07	2.49e-05	6.08e-07	2.49e-05	2.43e-05	2.55e-05
			All at once	2.53e-05	2.66e-06	2.46e-05	2.56e-06	2.46e-05	2.21e-05	2.74e-05
			One at a time	2.55e-05	2.77e-06	2.48e-05	2.65e-06	2.47e-05	2.22e-05	2.76e-05
	z=2 cm,4th column	enriched Li_2CO_3	Ref.	1.07e-05	3.43e-07	1.07e-05	3.43e-07	1.07e-05	1.04e-05	1.10e-05
			All at once	1.13e-05	1.61e-06	1.07e-05	1.52e-06	1.07e-05	9.22e-06	1.24e-05
			One at a time	1.13e-05	1.54e-06	1.07e-05	1.45e-06	1.06e-05	9.20e-06	1.24e-05
	z=2 cm,5th column	enriched Li_2CO_3	Ref.	5.78e-06	2.29e-07	5.78e-06	2.29e-07	5.78e-06	5.55e-06	6.01e-06
			All at once	6.46e-06	1.21e-06	5.89e-06	1.10e-06	5.90e-06	4.85e-06	7.15e-06
			One at a time	6.51e-06	1.29e-06	5.89e-06	1.13e-06	5.95e-06	4.83e-06	7.22e-06
^{7}Li(n,XT) on 95% ^{6}Li	z=2 cm,1st column	enriched Li_2CO_3	Ref.	6.42e-06	9.14e-08	6.42e-06	9.14e-08	6.42e-06	6.33e-06	6.51e-06
			All at once	6.93e-06	4.72e-07	6.86e-06	4.74e-07	6.91e-06	6.44e-06	7.37e-06
			One at a time	6.92e-06	4.46e-07	6.85e-06	4.49e-07	6.89e-06	6.43e-06	7.36e-06
	z=2 cm,2nd column	enriched Li_2CO_3	Ref.	4.50e-06	8.07e-08	4.50e-06	8.07e-08	4.50e-06	4.42e-06	4.58e-06
			All at once	4.60e-06	4.01e-07	4.52e-06	3.96e-07	4.53e-06	4.14e-06	4.93e-06
			One at a time	4.60e-06	3.95e-07	4.54e-06	3.88e-07	4.53e-06	4.13e-06	4.96e-06
	z=2 cm,3rd column	enriched Li_2CO_3	Ref.	2.07e-06	5.07e-08	2.07e-06	5.07e-08	2.07e-06	2.02e-06	2.12e-06
			All at once	2.11e-06	2.21e-07	2.05e-06	2.13e-07	2.05e-06	1.84e-06	2.28e-06
			One at a time	2.12e-06	2.31e-07	2.06e-06	2.21e-07	2.06e-06	1.85e-06	2.30e-06
	z=2 cm,4th column	enriched Li_2CO_3	Ref.	8.91e-07	2.85e-08	8.91e-07	2.85e-08	8.91e-07	8.62e-07	9.20e-07
			All at once	9.41e-07	1.34e-07	8.88e-07	1.27e-07	8.92e-07	7.68e-07	1.03e-06
			One at a time	9.38e-07	1.28e-07	8.92e-07	1.21e-07	8.85e-07	7.66e-07	1.03e-06
	z=2 cm,5th column	enriched Li_2CO_3	Ref.	4.81e-07	1.91e-08	4.81e-07	1.91e-08	4.81e-07	4.62e-07	5.01e-07
			All at once	5.38e-07	1.01e-07	4.91e-07	9.20e-08	4.91e-07	4.04e-07	5.96e-07
			One at a time	5.42e-07	1.07e-07	4.90e-07	9.45e-08	4.96e-07	4.02e-07	6.01e-07
Total flux	z=-2 cm,1st column	pure ^{93}Nb	Ref.	1.36e-03	3.92e-06	1.36e-03	3.92e-06	1.36e-03	1.36e-03	1.37e-03
			All at once	1.41e-03	3.25e-05	1.41e-03	3.27e-05	1.41e-03	1.39e-03	1.44e-03
			One at a time	1.41e-03	3.28e-05	1.41e-03	3.30e-05	1.42e-03	1.39e-03	1.44e-03
		pure ^{27}Al	Ref.	1.28e-03	3.79e-06	1.28e-03	3.79e-06	1.28e-03	1.28e-03	1.29e-03
			All at once	1.35e-03	4.20e-05	1.35e-03	4.25e-05	1.37e-03	1.27e-03	1.42e-03
			One at a time	1.36e-03	4.06e-05	1.36e-03	4.12e-05	1.37e-03	1.31e-03	1.42e-03
		^{nat}Ni	Ref.	1.24e-03	3.76e-06	1.24e-03	3.76e-06	1.24e-03	1.24e-03	1.25e-03
			All at once	1.32e-03	4.81e-05	1.31e-03	4.86e-05	1.34e-03	1.22e-03	1.39e-03
			One at a time	1.32e-03	4.65e-05	1.32e-03	4.72e-05	1.34e-03	1.28e-03	1.39e-03
		pure ^{115}In	Ref.	1.21e-03	3.68e-06	1.21e-03	3.68e-06	1.21e-03	1.21e-03	1.22e-03
			All at once	1.29e-03	4.85e-05	1.29e-03	4.91e-05	1.31e-03	1.19e-03	1.37e-03
			One at a time	1.30e-03	4.65e-05	1.30e-03	4.73e-05	1.32e-03	1.20e-03	1.37e-03
	z=-2 cm,2nd column	pure ^{93}Nb	Ref.	5.91e-04	2.64e-06	5.91e-04	2.64e-06	5.91e-04	5.89e-04	5.94e-04
			All at once	6.02e-04	1.81e-05	6.01e-04	1.81e-05	5.97e-04	5.81e-04	6.16e-04
			One at a time	6.00e-04	1.77e-05	6.00e-04	1.77e-05	5.96e-04	5.81e-04	6.15e-04
		pure ^{27}Al	Ref.	5.57e-04	2.57e-06	5.57e-04	2.57e-06	5.57e-04	5.54e-04	5.59e-04
			All at once	5.72e-04	2.38e-05	5.71e-04	2.36e-05	5.56e-04	5.43e-04	5.74e-04
			One at a time	5.71e-04	2.24e-05	5.70e-04	2.22e-05	5.56e-04	5.43e-04	5.74e-04
		^{nat}Ni	Ref.	5.33e-04	2.50e-06	5.33e-04	2.50e-06	5.33e-04	5.30e-04	5.35e-04
			All at once	5.51e-04	2.75e-05	5.50e-04	2.72e-05	5.31e-04	5.19e-04	5.45e-04
			One at a time	5.50e-04	2.60e-05	5.49e-04	2.58e-05	5.32e-04	5.20e-04	5.46e-04
		pure ^{115}In	Ref.	5.14e-04	2.45e-06	5.14e-04	2.45e-06	5.14e-04	5.11e-04	5.16e-04

(*continued on next page*)

Table C.2 (*continued*).

			All at once	5.37e-04	2.72e-05	5.35e-04	2.71e-05	5.17e-04	5.05e-04	5.31e-04
			One at a time	5.36e-04	2.63e-05	5.35e-04	2.61e-05	5.18e-04	5.06e-04	5.31e-04
	z=-2 cm,3rd column	pure ^{93}Nb	Ref.	2.83e-04	1.84e-06	2.83e-04	1.84e-06	2.83e-04	2.81e-04	2.84e-04
			All at once	2.90e-04	1.05e-05	2.89e-04	1.05e-05	2.88e-04	2.79e-04	2.99e-04
			One at a time	2.90e-04	1.01e-05	2.89e-04	1.01e-05	2.89e-04	2.79e-04	2.99e-04
		pure ^{27}Al	Ref.	2.65e-04	1.81e-06	2.65e-04	1.81e-06	2.65e-04	2.63e-04	2.67e-04
			All at once	2.75e-04	1.30e-05	2.74e-04	1.29e-05	2.70e-04	2.60e-04	2.85e-04
			One at a time	2.76e-04	1.27e-05	2.75e-04	1.26e-05	2.71e-04	2.61e-04	2.86e-04
		^{nat}Ni	Ref.	2.54e-04	1.73e-06	2.54e-04	1.73e-06	2.54e-04	2.52e-04	2.55e-04
			All at once	2.65e-04	1.46e-05	2.64e-04	1.45e-05	2.56e-04	2.48e-04	2.69e-04
			One at a time	2.65e-04	1.45e-05	2.64e-04	1.45e-05	2.58e-04	2.49e-04	2.71e-04
		pure ^{115}In	Ref.	2.49e-04	1.73e-06	2.49e-04	1.73e-06	2.49e-04	2.47e-04	2.51e-04
			All at once	2.59e-04	1.45e-05	2.58e-04	1.44e-05	2.50e-04	2.41e-04	2.66e-04
			One at a time	2.58e-04	1.41e-05	2.58e-04	1.40e-05	2.51e-04	2.42e-04	2.62e-04
	z=-2 cm,4th column	pure ^{93}Nb	Ref.	1.22e-04	1.19e-06	1.22e-04	1.19e-06	1.22e-04	1.20e-04	1.23e-04
			All at once	1.22e-04	5.44e-06	1.22e-04	5.42e-06	1.22e-04	1.16e-04	1.27e-04
			One at a time	1.23e-04	5.41e-06	1.23e-04	5.40e-06	1.23e-04	1.17e-04	1.28e-04
		pure ^{27}Al	Ref.	1.20e-04	1.21e-06	1.20e-04	1.21e-06	1.20e-04	1.19e-04	1.21e-04
			All at once	1.19e-04	6.00e-06	1.18e-04	5.98e-06	1.18e-04	1.12e-04	1.24e-04
			One at a time	1.20e-04	6.33e-06	1.19e-04	6.33e-06	1.19e-04	1.13e-04	1.25e-04
		^{nat}Ni	Ref.	1.15e-04	1.15e-06	1.15e-04	1.15e-06	1.15e-04	1.14e-04	1.16e-04
			All at once	1.16e-04	6.39e-06	1.15e-04	6.32e-06	1.14e-04	1.09e-04	1.20e-04
			One at a time	1.16e-04	6.93e-06	1.16e-04	6.87e-06	1.15e-04	1.09e-04	1.22e-04
		pure ^{115}In	Ref.	1.12e-04	1.14e-06	1.12e-04	1.14e-06	1.12e-04	1.11e-04	1.13e-04
			All at once	1.13e-04	6.31e-06	1.13e-04	6.27e-06	1.12e-04	1.06e-04	1.18e-04
			One at a time	1.14e-04	6.88e-06	1.13e-04	6.80e-06	1.12e-04	1.06e-04	1.18e-04
	z=-2 cm,5th column	pure ^{93}Nb	Ref.	5.72e-05	8.23e-07	5.72e-05	8.23e-07	5.72e-05	5.64e-05	5.80e-05
			All at once	5.78e-05	3.53e-06	5.74e-05	3.53e-06	5.75e-05	5.37e-05	6.13e-05
			One at a time	5.76e-05	3.61e-06	5.72e-05	3.57e-06	5.71e-05	5.35e-05	6.10e-05
		pure ^{27}Al	Ref.	5.58e-05	8.16e-07	5.58e-05	8.16e-07	5.58e-05	5.50e-05	5.66e-05
			All at once	5.60e-05	3.74e-06	5.56e-05	3.69e-06	5.54e-05	5.17e-05	5.93e-05
			One at a time	5.57e-05	3.84e-06	5.53e-05	3.81e-06	5.51e-05	5.12e-05	5.93e-05
		^{nat}Ni	Ref.	5.35e-05	7.81e-07	5.35e-05	7.81e-07	5.35e-05	5.27e-05	5.43e-05
			All at once	5.43e-05	3.77e-06	5.39e-05	3.75e-06	5.38e-05	5.02e-05	5.76e-05
			One at a time	5.42e-05	3.82e-06	5.38e-05	3.83e-06	5.36e-05	5.00e-05	5.75e-05
		pure ^{115}In	Ref.	5.18e-05	7.80e-07	5.18e-05	7.80e-07	5.18e-05	5.10e-05	5.26e-05
			All at once	5.30e-05	3.81e-06	5.26e-05	3.77e-06	5.24e-05	4.88e-05	5.63e-05
			One at a time	5.28e-05	3.84e-06	5.24e-05	3.79e-06	5.22e-05	4.86e-05	5.60e-05
^{93}Nb(n,2n) on ^{93}Nb	z=-2 cm,1st column	pure ^{93}Nb	Ref.	1.14e-04	5.11e-07	1.14e-04	5.11e-07	1.14e-04	1.14e-04	1.15e-04
			All at once	1.14e-04	3.42e-06	1.14e-04	3.42e-06	1.14e-04	1.11e-04	1.17e-04
			One at a time	1.14e-04	3.47e-06	1.14e-04	3.47e-06	1.14e-04	1.11e-04	1.17e-04
	z=-2 cm,2nd column	pure ^{93}Nb	Ref.	1.77e-05	1.99e-07	1.77e-05	1.99e-07	1.77e-05	1.75e-05	1.79e-05
			All at once	1.76e-05	9.35e-07	1.76e-05	9.31e-07	1.76e-05	1.66e-05	1.86e-05
			One at a time	1.76e-05	8.75e-07	1.76e-05	8.73e-07	1.76e-05	1.67e-05	1.85e-05
	z=-2 cm,3rd column	pure ^{93}Nb	Ref.	4.28e-06	1.02e-07	4.28e-06	1.02e-07	4.28e-06	4.18e-06	4.38e-06
			All at once	4.17e-06	4.17e-07	4.11e-06	4.10e-07	4.10e-06	3.68e-06	4.55e-06
			One at a time	4.17e-06	4.34e-07	4.11e-06	4.29e-07	4.11e-06	3.67e-06	4.56e-06
	z=-2 cm,4th column	pure ^{93}Nb	Ref.	7.55e-07	4.62e-08	7.55e-07	4.62e-08	7.55e-07	7.09e-07	8.01e-07
			All at once	8.29e-07	1.89e-07	7.74e-07	1.82e-07	7.75e-07	5.93e-07	9.74e-07
			One at a time	8.31e-07	1.80e-07	7.80e-07	1.69e-07	7.73e-07	6.02e-07	9.63e-07
	z=-2 cm,5th column	pure ^{93}Nb	Ref.	2.26e-07	2.20e-08	2.26e-07	2.20e-08	2.26e-07	2.04e-07	2.48e-07
			All at once	2.44e-07	9.98e-08	2.44e-07	9.98e-08	1.99e-07	1.07e-07	3.05e-07
			One at a time	2.38e-07	1.02e-07	1.85e-07	9.26e-08	1.94e-07	1.06e-07	2.92e-07
^{27}Al(n,α)on^{27}Al	z=-2 cm,1st column	pure ^{27}Al	Ref.	2.80e-05	1.25e-07	2.80e-05	1.25e-07	2.80e-05	2.79e-05	2.82e-05
			All at once	2.83e-05	8.67e-07	2.82e-05	8.67e-07	2.83e-05	2.75e-05	2.90e-05
			One at a time	2.83e-05	8.72e-07	2.83e-05	8.74e-07	2.83e-05	2.76e-05	2.90e-05
	z=-2 cm,2nd column	pure ^{27}Al	Ref.	4.52e-06	5.02e-08	4.52e-06	5.02e-08	4.52e-06	4.46e-06	4.57e-06
			All at once	4.54e-06	2.42e-07	4.52e-06	2.41e-07	4.52e-06	4.28e-06	4.77e-06
			One at a time	4.53e-06	2.39e-07	4.51e-06	2.39e-07	4.51e-06	4.27e-06	4.76e-06
	z=-2 cm,3rd column	pure ^{27}Al	Ref.	1.11e-06	2.65e-08	1.11e-06	2.65e-08	1.11e-06	1.08e-06	1.13e-06
			All at once	1.09e-06	1.09e-07	1.07e-06	1.07e-07	1.07e-06	9.64e-07	1.19e-06
			One at a time	1.09e-06	1.11e-07	1.08e-06	1.09e-07	1.08e-06	9.65e-07	1.19e-06
	z=-2 cm,4th column	pure ^{27}Al	Ref.	2.01e-07	1.10e-08	2.01e-07	1.10e-08	2.01e-07	1.90e-07	2.12e-07
			All at once	2.22e-07	4.89e-08	2.08e-07	4.75e-08	2.08e-07	1.61e-07	2.61e-07
			One at a time	2.23e-07	4.77e-08	2.09e-07	4.47e-08	2.06e-07	1.61e-07	2.57e-07
	z=-2 cm,5th column	pure ^{27}Al	Ref.	6.63e-08	7.02e-09	6.63e-08	7.02e-09	6.63e-08	5.93e-08	7.34e-08
			All at once	6.58e-08	2.63e-08	9.93e-13	8.80e-11	5.43e-08	3.03e-08	8.20e-08
			One at a time	6.47e-08	2.67e-08	5.02e-08	2.47e-08	5.28e-08	3.10e-08	7.81e-08

(continued on next page)

Table C.2 (*continued*).

$^{58}Ni(n,2n)$ on ^{nat}Ni	z=-2 cm,1st column	^{nat}Ni	Ref.	7.95e-06	3.67e-08	7.95e-06	3.67e-08	7.95e-06	7.92e-06	7.99e-06
			All at once	7.95e-06	2.61e-07	7.94e-06	2.61e-07	7.97e-06	7.73e-06	8.18e-06
			One at a time	8.00e-06	2.55e-07	7.99e-06	2.55e-07	7.99e-06	7.76e-06	8.21e-06
	z=-2 cm,2nd column	^{nat}Ni	Ref.	1.17e-06	1.42e-08	1.17e-06	1.42e-08	1.17e-06	1.15e-06	1.18e-06
			All at once	1.17e-06	6.68e-08	1.16e-06	6.65e-08	1.16e-06	1.10e-06	1.23e-06
			One at a time	1.17e-06	6.34e-08	1.17e-06	6.31e-08	1.17e-06	1.10e-06	1.23e-06
	z=-2 cm,3rd column	^{nat}Ni	Ref.	2.62e-07	6.51e-09	2.62e-07	6.51e-09	2.62e-07	2.56e-07	2.69e-07
			All at once	2.65e-07	2.88e-08	2.61e-07	2.87e-08	2.61e-07	2.32e-07	2.92e-07
			One at a time	2.66e-07	3.00e-08	2.61e-07	2.95e-08	2.61e-07	2.32e-07	2.92e-07
	z=-2 cm,4th column	^{nat}Ni	Ref.	4.83e-08	3.42e-09	4.83e-08	3.42e-09	4.83e-08	4.49e-08	5.17e-08
			All at once	5.14e-08	1.26e-08	4.78e-08	1.22e-08	4.78e-08	3.56e-08	6.14e-08
			One at a time	5.09e-08	1.20e-08	4.73e-08	1.20e-08	4.75e-08	3.56e-08	6.06e-08
	z=-2 cm,5th column	^{nat}Ni	Ref.	1.35e-08	1.47e-09	1.35e-08	1.47e-09	1.35e-08	1.20e-08	1.50e-08
			All at once	1.46e-08	6.49e-09	1.46e-08	6.49e-09	1.14e-08	5.47e-09	1.84e-08
			One at a time	1.43e-08	6.46e-09	1.43e-08	6.46e-09	1.11e-08	5.10e-09	1.82e-08
$^{58}Ni(n,p)$ on ^{nat}Ni	z=-2 cm,1st column	^{nat}Ni	Ref.	1.14e-04	5.46e-07	1.14e-04	5.46e-07	1.14e-04	1.14e-04	1.15e-04
			All at once	1.18e-04	4.44e-06	1.18e-04	4.43e-06	1.17e-04	1.13e-04	1.22e-04
			One at a time	1.18e-04	4.51e-06	1.18e-04	4.51e-06	1.18e-04	1.14e-04	1.22e-04
	z=-2 cm,2nd column	^{nat}Ni	Ref.	2.32e-05	2.48e-07	2.32e-05	2.48e-07	2.32e-05	2.30e-05	2.35e-05
			All at once	2.37e-05	1.35e-06	2.36e-05	1.33e-06	2.35e-05	2.23e-05	2.48e-05
			One at a time	2.37e-05	1.22e-06	2.35e-05	1.20e-06	2.35e-05	2.23e-05	2.48e-05
	z=-2 cm,3rd column	^{nat}Ni	Ref.	6.31e-06	1.21e-07	6.31e-06	1.21e-07	6.31e-06	6.19e-06	6.43e-06
			All at once	6.56e-06	6.06e-07	6.44e-06	5.93e-07	6.44e-06	5.87e-06	7.06e-06
			One at a time	6.58e-06	6.23e-07	6.44e-06	6.14e-07	6.46e-06	5.86e-06	7.09e-06
	z=-2 cm,4th column	^{nat}Ni	Ref.	1.57e-06	6.62e-08	1.57e-06	6.62e-08	1.57e-06	1.51e-06	1.64e-06
			All at once	1.52e-06	2.71e-07	1.43e-06	2.52e-07	1.43e-06	1.19e-06	1.71e-06
			One at a time	1.53e-06	2.63e-07	1.44e-06	2.44e-07	1.44e-06	1.19e-06	1.70e-06
	z=-2 cm,5th column	^{nat}Ni	Ref.	4.75e-07	3.76e-08	4.75e-07	3.76e-08	4.75e-07	4.37e-07	5.13e-07
			All at once	4.80e-07	1.45e-07	4.06e-07	1.28e-07	4.09e-07	2.92e-07	5.50e-07
			One at a time	4.80e-07	1.49e-07	3.99e-07	1.34e-07	4.15e-07	2.92e-07	5.56e-07
$^{197}Au(n,2n)$ on ^{197}Au	z=-2 cm1st column	pure ^{197}Au	Ref.	1.43e-05	7.15e-08	1.43e-05	7.15e-08	1.43e-05	1.42e-05	1.44e-05
			All at once	1.45e-05	5.43e-07	1.45e-05	5.31e-07	1.45e-05	1.40e-05	1.50e-05
			One at a time	1.45e-05	5.43e-07	1.45e-05	5.30e-07	1.45e-05	1.40e-05	1.50e-05
	z=-2 cm,2nd column	pure ^{197}Au	Ref.	2.26e-06	2.70e-08	2.26e-06	2.70e-08	2.26e-06	2.23e-06	2.29e-06
			All at once	2.25e-06	1.45e-07	2.23e-06	1.38e-07	2.23e-06	2.10e-06	2.37e-06
			One at a time	2.26e-06	1.42e-07	2.24e-06	1.33e-07	2.24e-06	2.11e-06	2.37e-06
	z=-2 cm,3rd column	pure ^{197}Au	Ref.	5.20e-07	1.28e-08	5.20e-07	1.28e-08	5.20e-07	5.07e-07	5.33e-07
			All at once	5.33e-07	6.49e-08	5.22e-07	5.68e-08	5.22e-07	4.65e-07	5.81e-07
			One at a time	5.30e-07	6.16e-08	5.19e-07	5.79e-08	5.17e-07	4.60e-07	5.79e-07
	z=-2 cm,4th column	pure ^{197}Au	Ref.	9.22e-08	5.17e-09	9.22e-08	5.17e-09	9.22e-08	8.71e-08	9.74e-08
			All at once	1.08e-07	2.76e-08	1.00e-07	2.43e-08	9.95e-08	7.58e-08	1.27e-07
			One at a time	1.06e-07	2.40e-08	9.95e-08	2.29e-08	9.94e-08	7.66e-08	1.24e-07
	z=-2 cm,5th column	pure ^{197}Au	Ref.	2.91e-08	2.92e-09	2.91e-08	2.92e-09	2.91e-08	2.62e-08	3.20e-08
			All at once	3.20e-08	1.45e-08	3.20e-08	1.45e-08	2.56e-08	1.33e-08	3.97e-08
			One at a time	3.15e-08	1.86e-08	8.19e-10	4.60e-09	2.46e-08	1.38e-08	3.71e-08
$^{197}Au(n,\gamma)$ on ^{197}Au	z=-2 cm,1st column	pure ^{197}Au	Ref.	1.12e-04	5.96e-06	1.12e-04	5.96e-06	1.12e-04	1.06e-04	1.18e-04
			All at once	1.19e-04	3.11e-05	9.82e-05	2.57e-05	9.86e-05	7.59e-05	1.30e-04
			One at a time	1.19e-04	3.02e-05	9.77e-05	2.66e-05	1.01e-04	7.63e-05	1.32e-04
	z=-2 cm,2nd column	pure ^{197}Au	Ref.	7.84e-05	5.39e-06	7.84e-05	5.39e-06	7.84e-05	7.30e-05	8.38e-05
			All at once	8.39e-05	2.57e-05	6.40e-05	2.05e-05	6.55e-05	4.74e-05	9.07e-05
			One at a time	8.26e-05	2.62e-05	6.27e-05	2.00e-05	6.45e-05	4.79e-05	8.69e-05
	z=-2 cm,3rd column	pure ^{197}Au	Ref.	4.04e-05	3.92e-06	4.04e-05	3.92e-06	4.04e-05	3.65e-05	4.43e-05
			All at once	4.05e-05	1.71e-05	2.45e-05	1.08e-05	2.55e-05	1.07e-05	6.59e-05
			One at a time	3.92e-05	1.80e-05	2.32e-05	1.01e-05	2.38e-05	1.02e-05	6.16e-05
	z=-2 cm,4th column	pure ^{197}Au	Ref.	1.85e-05	2.31e-06	1.85e-05	2.31e-06	1.84e-05	1.61e-05	2.08e-05
			All at once	1.77e-05	1.10e-05	8.21e-06	4.08e-06	8.26e-06	3.13e-06	2.55e-05
			One at a time	1.89e-05	1.14e-05	8.19e-06	4.50e-06	9.07e-06	2.94e-06	2.78e-05
	z=-2 cm,5th column	pure ^{197}Au	Ref.	1.52e-05	3.99e-06	1.52e-05	3.99e-06	1.52e-05	1.12e-05	1.91e-05
			All at once	1.03e-05	8.47e-06	3.57e-06	2.02e-06	3.51e-06	1.16e-06	1.19e-05
			One at a time	1.06e-05	8.42e-06	3.54e-06	2.10e-06	3.59e-06	1.19e-06	1.30e-05
$^{115}In(n,n')$ on ^{115}In	z=-2 cm,1st column	pure ^{115}In	Ref.	1.01e-04	5.12e-07	1.01e-04	5.12e-07	1.01e-04	1.00e-04	1.01e-04
			All at once	1.08e-04	5.16e-06	1.08e-04	5.19e-06	1.10e-04	1.04e-04	1.14e-04
			One at a time	1.08e-04	4.97e-06	1.08e-04	5.01e-06	1.10e-04	1.05e-04	1.14e-04
	z=-2 cm,2nd column	pure ^{115}In	Ref.	3.05e-05	2.77e-07	3.05e-05	2.77e-07	3.05e-05	3.02e-05	3.07e-05
			All at once	3.16e-05	2.02e-06	3.14e-05	2.00e-06	3.08e-05	2.94e-05	3.26e-05
			One at a time	3.15e-05	1.87e-06	3.13e-05	1.85e-06	3.08e-05	2.94e-05	3.25e-05
	z=-2 cm,3rd column	pure ^{115}In	Ref.	1.09e-05	1.62e-07	1.09e-05	1.62e-07	1.09e-05	1.08e-05	1.11e-05

(continued on next page)

Table C.2 (*continued*).

		All at once	1.13e-05	9.07e-07	1.11e-05	9.00e-07	1.11e-05	1.02e-05	1.20e-05
		One at a time	1.12e-05	8.93e-07	1.11e-05	8.92e-07	1.11e-05	1.03e-05	1.19e-05
z=-2 cm,4th column	pure ^{115}In	Ref.	3.48e-06	8.68e-08	3.48e-06	8.68e-08	3.48e-06	3.40e-06	3.57e-06
		All at once	3.33e-06	3.79e-07	3.23e-06	3.77e-07	3.26e-06	2.88e-06	3.65e-06
		One at a time	3.33e-06	3.97e-07	3.23e-06	3.91e-07	3.27e-06	2.91e-06	3.65e-06
z=-2 cm,5th column	pure ^{115}In	Ref.	1.14e-06	4.29e-08	1.14e-06	4.29e-08	1.14e-06	1.10e-06	1.18e-06
		All at once	1.20e-06	2.06e-07	1.13e-06	1.94e-07	1.13e-06	9.41e-07	1.34e-06
		One at a time	1.20e-06	2.20e-07	1.12e-06	2.10e-07	1.13e-06	9.19e-07	1.37e-06

Table C.3
Sensitivity/uncertainty coefficients for ^{6}Li(n,T) on ^{nat}Li on front Li_2CO_3 in dosimeter pack at z = 2 cm, 1st column. FENDL-3.2b nuclear data libraries used for transport, IRDFF-II nuclear data libraries for reaction rate tallying.

		All at once	Dosimeter pack at z=2 cm, 1st column	Dosimeter pack at z=2 cm, 2nd column	Dosimeter pack at z=2 cm, 3rd column	Dosimeter pack at z=2 cm, 4th column	Dosimeter pack at z=2 cm, 5th column	Dosimeter pack at z=-2 cm, 1st column	Dosimeter pack at z=-2 cm, 2nd column	Dosimeter pack at z=-2 cm, 3rd column	Dosimeter pack at z=-2 cm, 4th column	Dosimeter pack at z=-2 cm, 5th column	Source perturbation
Perturbed unit	Direction	[per Dir.]	[per Dir.]	[per Dir.]	[per Dir.]	[per Dir.]	[per Dir.]	[per Dir.]	[per Dir.]	[per Dir.]	[per Dir.]	[per Dir.]	[per Dir.]
Dosimeter pack at z=2 cm,1st column	x [mm]	1.02e-08	1.43e-08	0.00e +00	0.00e +00	0.00e +00	0.00e +00	0.00e +00	0.00e +00	0.00e +00	0.00e +00	0.00e +00	0.00e +00
	y [mm]	1.60e-08	-8.16e-09	0.00e +00	0.00e +00	0.00e +00	0.00e +00	0.00e +00	0.00e +00	0.00e +00	0.00e +00	0.00e +00	0.00e +00
	z [mm]	-1.72e-07	-1.40e-07	0.00e +00	0.00e +00	0.00e +00	0.00e +00	0.00e +00	0.00e +00	0.00e +00	0.00e +00	0.00e +00	0.00e +00
Dosimeter pack at z=2 cm,2nd column	x [mm]	8.02e-09	0.00e +00	-3.85e-08	0.00e +00	0.00e +00	0.00e +00	0.00e +00	0.00e +00	0.00e +00	0.00e +00	0.00e +00	0.00e +00
	y [mm]	9.57e-09	0.00e +00	1.19e-09	0.00e +00	0.00e +00	0.00e +00	0.00e +00	0.00e +00	0.00e +00	0.00e +00	0.00e +00	0.00e +00
	z [mm]	8.63e-09	0.00e +00	-4.42e-09	0.00e +00	0.00e +00	0.00e +00	0.00e +00	0.00e +00	0.00e +00	0.00e +00	0.00e +00	0.00e +00
Dosimeter pack at z=2 cm,3rd column	x [mm]	-2.65e-09	0.00e +00	0.00e +00	1.32e-08	0.00e +00	0.00e +00	0.00e +00	0.00e +00	0.00e +00	0.00e +00	0.00e +00	0.00e +00
	y [mm]	1.42e-08	0.00e +00	0.00e +00	4.17e-08	0.00e +00	0.00e +00	0.00e +00	0.00e +00	0.00e +00	0.00e +00	0.00e +00	0.00e +00
	z [mm]	-4.67e-09	0.00e +00	0.00e +00	-3.90e-08	0.00e +00	0.00e +00	0.00e +00	0.00e +00	0.00e +00	0.00e +00	0.00e +00	0.00e +00
Dosimeter pack at z=2 cm,4th column	x [mm]	-7.92e-09	0.00e +00	0.00e +00	0.00e +00	-5.91e-10	0.00e +00	0.00e +00	0.00e +00	0.00e +00	0.00e +00	0.00e +00	0.00e +00
	y [mm]	4.01e-09	0.00e +00	0.00e +00	0.00e +00	9.62e-09	0.00e +00	0.00e +00	0.00e +00	0.00e +00	0.00e +00	0.00e +00	0.00e +00
	z [mm]	7.98e-09	0.00e +00	0.00e +00	0.00e +00	-3.91e-09	0.00e +00	0.00e +00	0.00e +00	0.00e +00	0.00e +00	0.00e +00	0.00e +00
Dosimeter pack at z=2 cm,5th column	x [mm]	-1.47e-08	0.00e +00	0.00e +00	0.00e +00	0.00e +00	-3.18e-08	0.00e +00	0.00e +00	0.00e +00	0.00e +00	0.00e +00	0.00e +00
	y [mm]	-2.25e-08	0.00e +00	0.00e +00	0.00e +00	0.00e +00	-1.37e-08	0.00e +00	0.00e +00	0.00e +00	0.00e +00	0.00e +00	0.00e +00
	z [mm]	6.48e-09	0.00e +00	0.00e +00	0.00e +00	0.00e +00	-1.90e-08	0.00e +00	0.00e +00	0.00e +00	0.00e +00	0.00e +00	0.00e +00
Dosimeter pack at z=-2 cm,1st column	x [mm]	-3.87e-08	0.00e +00	0.00e +00	0.00e +00	0.00e +00	0.00e +00	7.42e-09	0.00e +00	0.00e +00	0.00e +00	0.00e +00	0.00e +00
	y [mm]	1.23e-09	0.00e +00	0.00e +00	0.00e +00	0.00e +00	0.00e +00	6.99e-09	0.00e +00	0.00e +00	0.00e +00	0.00e +00	0.00e +00
	z [mm]	3.13e-08	0.00e +00	0.00e +00	0.00e +00	0.00e +00	0.00e +00	1.42e-08	0.00e +00	0.00e +00	0.00e +00	0.00e +00	0.00e +00
Dosimeter pack at z=-2 cm,2nd column	x [mm]	-1.86e-08	0.00e +00	0.00e +00	0.00e +00	0.00e +00	0.00e +00	0.00e +00	-4.82e-08	0.00e +00	0.00e +00	0.00e +00	0.00e +00
	y [mm]	1.25e-08	0.00e +00	0.00e +00	0.00e +00	0.00e +00	0.00e +00	0.00e +00	-5.08e-08	0.00e +00	0.00e +00	0.00e +00	0.00e +00
	z [mm]	-1.33e-08	0.00e +00	0.00e +00	0.00e +00	0.00e +00	0.00e +00	0.00e +00	-1.55e-08	0.00e +00	0.00e +00	0.00e +00	0.00e +00
Dosimeter pack at z=-2 cm,3rd column	x [mm]	-3.60e-09	0.00e +00	0.00e +00	0.00e +00	0.00e +00	0.00e +00	0.00e +00	0.00e +00	-2.67e-08	0.00e +00	0.00e +00	0.00e +00
	y [mm]	1.97e-08	0.00e +00	0.00e +00	0.00e +00	0.00e +00	0.00e +00	0.00e +00	0.00e +00	-1.19e-08	0.00e +00	0.00e +00	0.00e +00
	z [mm]	-2.12e-08	0.00e +00	0.00e +00	0.00e +00	0.00e +00	0.00e +00	0.00e +00	0.00e +00	-1.30e-08	0.00e +00	0.00e +00	0.00e +00
Dosimeter pack at z=-2 cm,4th column	x [mm]	5.51e-09	0.00e +00	0.00e +00	0.00e +00	0.00e +00	0.00e +00	0.00e +00	0.00e +00	0.00e +00	5.38e-09	0.00e +00	0.00e +00
	y [mm]	-1.00e-08	0.00e +00	0.00e +00	0.00e +00	0.00e +00	0.00e +00	0.00e +00	0.00e +00	0.00e +00	5.03e-10	0.00e +00	0.00e +00
	z [mm]	-7.98e-10	0.00e +00	0.00e +00	0.00e +00	0.00e +00	0.00e +00	0.00e +00	0.00e +00	0.00e +00	-3.68e-08	0.00e +00	0.00e +00
Dosimeter pack at z=-2 cm,5th column	x [mm]	-1.97e-08	0.00e +00	0.00e +00	0.00e +00	0.00e +00	0.00e +00	0.00e +00	0.00e +00	0.00e +00	0.00e +00	7.15e-09	0.00e +00
	y [mm]	-2.30e-08	0.00e +00	0.00e +00	0.00e +00	0.00e +00	0.00e +00	0.00e +00	0.00e +00	0.00e +00	0.00e +00	2.58e-08	0.00e +00

(*continued on next page*)

Table C.3 (*continued*).

	z [mm]	-2.30e-08	0.00e +00	0.00e +00	0.00e +00	0.00e +00	0.00e +00	0.00e +00	0.00e +00	0.00e +00	0.00e +00	4.15e-08	0.00e +00
Source position	x [mm]	-7.90e-09	0.00e +00	0.00e +00	0.00e +00	0.00e +00	0.00e +00	0.00e +00	0.00e +00	0.00e +00	0.00e +00	0.00e +00	-3.36e-09
	z [mm]	5.63e-09	0.00e +00	0.00e +00	0.00e +00	0.00e +00	0.00e +00	0.00e +00	0.00e +00	0.00e +00	0.00e +00	0.00e +00	1.20e-08
Source direction	x dir. ref(0,1,0)	-7.99e-10	0.00e +00	0.00e +00	0.00e +00	0.00e +00	0.00e +00	0.00e +00	0.00e +00	0.00e +00	0.00e +00	0.00e +00	2.42e-08
	z dir. ref(0,1,0)	1.70e-08	0.00e +00	0.00e +00	0.00e +00	0.00e +00	0.00e +00	0.00e +00	0.00e +00	0.00e +00	0.00e +00	0.00e +00	3.96e-08
Const		8.60e-06	8.59e-06	8.08e-06	8.09e-06	8.08e-06	8.10e-06	8.10e-06	8.09e-06	8.12e-06	8.07e-06	8.07e-06	8.05e-06

Table C.4
Sensitivity/uncertainty coefficients for ^{6}Li(n,T) on ^{nat}Li on front Li_2CO_3 in dosimeter pack at z = 2 cm, 5th column. FENDL-3.2b nuclear data libraries used for transport, IRDFF-II nuclear data libraries for reaction rate tallying.

Perturbed unit	Direction	All at once [per Dir.]	Dosimeter pack at z=2 cm, 1st column [per Dir.]	Dosimeter pack at z=2 cm, 2nd column [per Dir.]	Dosimeter pack at z=2 cm, 3rd column [per Dir.]	Dosimeter pack at z=2 cm, 4th column [per Dir.]	Dosimeter pack at z=2 cm, 5th column [per Dir.]	Dosimeter pack at z=-2 cm, 1st column [per Dir.]	Dosimeter pack at z=-2 cm, 2nd column [per Dir.]	Dosimeter pack at z=-2 cm, 3rd column [per Dir.]	Dosimeter pack at z=-2 cm, 4th column [per Dir.]	Dosimeter pack at z=-2 cm, 5th column [per Dir.]	Source perturbation [per Dir.]
Dosimeter pack at z=2 cm,1st column	x [mm]	-1.42e-10	-3.93e-09	0.00e +00	0.00e +00	0.00e +00	0.00e +00	0.00e +00	0.00e +00	0.00e +00	0.00e +00	0.00e +00	0.00e +00
	y [mm]	1.54e-09	-5.45e-09	0.00e +00	0.00e +00	0.00e +00	0.00e +00	0.00e +00	0.00e +00	0.00e +00	0.00e +00	0.00e +00	0.00e +00
	z [mm]	-6.41e-10	6.26e-10	0.00e +00	0.00e +00	0.00e +00	0.00e +00	0.00e +00	0.00e +00	0.00e +00	0.00e +00	0.00e +00	0.00e +00
Dosimeter pack at z=2 cm,2nd column	x [mm]	-2.64e-09	0.00e +00	-5.43e-09	0.00e +00	0.00e +00	0.00e +00	0.00e +00	0.00e +00	0.00e +00	0.00e +00	0.00e +00	0.00e +00
	y [mm]	-3.04e-09	0.00e +00	-4.02e-09	0.00e +00	0.00e +00	0.00e +00	0.00e +00	0.00e +00	0.00e +00	0.00e +00	0.00e +00	0.00e +00
	z [mm]	-7.50e-09	0.00e +00	-5.31e-09	0.00e +00	0.00e +00	0.00e +00	0.00e +00	0.00e +00	0.00e +00	0.00e +00	0.00e +00	0.00e +00
Dosimeter pack at z=2 cm,3rd column	x [mm]	1.61e-09	0.00e +00	0.00e +00	-6.40e-11	0.00e +00	0.00e +00	0.00e +00	0.00e +00	0.00e +00	0.00e +00	0.00e +00	0.00e +00
	y [mm]	1.67e-09	0.00e +00	0.00e +00	-4.70e-09	0.00e +00	0.00e +00	0.00e +00	0.00e +00	0.00e +00	0.00e +00	0.00e +00	0.00e +00
	z [mm]	-1.91e-09	0.00e +00	0.00e +00	-3.17e-09	0.00e +00	0.00e +00	0.00e +00	0.00e +00	0.00e +00	0.00e +00	0.00e +00	0.00e +00
Dosimeter pack at z=2 cm,4th column	x [mm]	-5.38e-09	0.00e +00	0.00e +00	0.00e +00	-1.44e-08	0.00e +00	0.00e +00	0.00e +00	0.00e +00	0.00e +00	0.00e +00	0.00e +00
	y [mm]	4.45e-11	0.00e +00	0.00e +00	0.00e +00	3.94e-10	0.00e +00	0.00e +00	0.00e +00	0.00e +00	0.00e +00	0.00e +00	0.00e +00
	z [mm]	-5.30e-10	0.00e +00	0.00e +00	0.00e +00	2.99e-09	0.00e +00	0.00e +00	0.00e +00	0.00e +00	0.00e +00	0.00e +00	0.00e +00
Dosimeter pack at z=2 cm,5th column	x [mm]	-8.58e-10	0.00e +00	0.00e +00	0.00e +00	0.00e +00	1.24e-08	0.00e +00	0.00e +00	0.00e +00	0.00e +00	0.00e +00	0.00e +00
	y [mm]	-3.61e-09	0.00e +00	0.00e +00	0.00e +00	0.00e +00	-4.26e-09	0.00e +00	0.00e +00	0.00e +00	0.00e +00	0.00e +00	0.00e +00
	z [mm]	-1.19e-08	0.00e +00	0.00e +00	0.00e +00	0.00e +00	-1.87e-08	0.00e +00	0.00e +00	0.00e +00	0.00e +00	0.00e +00	0.00e +00
Dosimeter pack at z=-2 cm,1st column	x [mm]	-8.69e-09	0.00e +00	0.00e +00	0.00e +00	0.00e +00	0.00e +00	-7.60e-09	0.00e +00	0.00e +00	0.00e +00	0.00e +00	0.00e +00
	y [mm]	-4.71e-09	0.00e +00	0.00e +00	0.00e +00	0.00e +00	0.00e +00	-5.76e-09	0.00e +00	0.00e +00	0.00e +00	0.00e +00	0.00e +00
	z [mm]	1.29e-10	0.00e +00	0.00e +00	0.00e +00	0.00e +00	0.00e +00	-6.48e-09	0.00e +00	0.00e +00	0.00e +00	0.00e +00	0.00e +00
Dosimeter pack at z=-2 cm,2nd column	x [mm]	-3.75e-09	0.00e +00	0.00e +00	0.00e +00	0.00e +00	0.00e +00	0.00e +00	-6.08e-09	0.00e +00	0.00e +00	0.00e +00	0.00e +00
	y [mm]	-7.24e-09	0.00e +00	0.00e +00	0.00e +00	0.00e +00	0.00e +00	0.00e +00	-2.99e-09	0.00e +00	0.00e +00	0.00e +00	0.00e +00
	z [mm]	-1.98e-09	0.00e +00	0.00e +00	0.00e +00	0.00e +00	0.00e +00	0.00e +00	7.71e-10	0.00e +00	0.00e +00	0.00e +00	0.00e +00
Dosimeter pack at z=-2 cm,3rd column	x [mm]	-4.01e-09	0.00e +00	0.00e +00	0.00e +00	0.00e +00	0.00e +00	0.00e +00	0.00e +00	-5.07e-10	0.00e +00	0.00e +00	0.00e +00
	y [mm]	-3.95e-09	0.00e +00	0.00e +00	0.00e +00	0.00e +00	0.00e +00	0.00e +00	0.00e +00	2.51e-10	0.00e +00	0.00e +00	0.00e +00
	z [mm]	-6.14e-09	0.00e +00	0.00e +00	0.00e +00	0.00e +00	0.00e +00	0.00e +00	0.00e +00	-2.58e-09	0.00e +00	0.00e +00	0.00e +00

(*continued on next page*)

Table C.4 (*continued*).

Dosimeter pack at z=-2 cm,4th column	x [mm]	-3.40e-09	0.00e +00	0.00e +00	0.00e +00	0.00e +00	0.00e +00	0.00e +00	0.00e +00	0.00e +00	-8.35e-10	0.00e +00	0.00e +00
	y [mm]	-1.46e-09	0.00e +00	0.00e +00	0.00e +00	0.00e +00	0.00e +00	0.00e +00	0.00e +00	0.00e +00	-4.63e-11	0.00e +00	0.00e +00
	z [mm]	-1.51e-10	0.00e +00	0.00e +00	0.00e +00	0.00e +00	0.00e +00	0.00e +00	0.00e +00	0.00e +00	-3.42e-10	0.00e +00	0.00e +00
Dosimeter pack at z=-2 cm,5th column	x [mm]	-3.55e-10	0.00e +00	0.00e +00	0.00e +00	0.00e +00	0.00e +00	0.00e +00	0.00e +00	0.00e +00	0.00e +00	1.97e-09	0.00e +00
	y [mm]	-3.18e-09	0.00e +00	0.00e +00	0.00e +00	0.00e +00	0.00e +00	0.00e +00	0.00e +00	0.00e +00	0.00e +00	-1.82e-09	0.00e +00
	z [mm]	-5.64e-09	0.00e +00	0.00e +00	0.00e +00	0.00e +00	0.00e +00	0.00e +00	0.00e +00	0.00e +00	0.00e +00	-2.86e-08	0.00e +00
Source position	x [mm]	-2.03e-10	0.00e +00	0.00e +00	0.00e +00	0.00e +00	0.00e +00	0.00e +00	0.00e +00	0.00e +00	0.00e +00	0.00e +00	2.41e-09
	z [mm]	-8.58e-10	0.00e +00	0.00e +00	0.00e +00	0.00e +00	0.00e +00	0.00e +00	0.00e +00	0.00e +00	0.00e +00	0.00e +00	4.04e-09
Source direction	x dir. ref(0,1,0)	2.54e-10	0.00e +00	0.00e +00	0.00e +00	0.00e +00	0.00e +00	0.00e +00	0.00e +00	0.00e +00	0.00e +00	0.00e +00	-6.03e-09
	z dir. ref(0,1,0)	-4.42e-09	0.00e +00	0.00e +00	0.00e +00	0.00e +00	0.00e +00	0.00e +00	0.00e +00	0.00e +00	0.00e +00	0.00e +00	-1.19e-08
Const		6.73e-07	6.61e-07	6.65e-07	6.58e-07	6.60e-07	6.67e-07	6.68e-07	6.69e-07	6.63e-07	6.63e-07	6.77e-07	6.61e-07

References

[1] G. Federici, L. Boccaccini, F. Cismondi, M. Gasparotto, Y. Poitevin, I. Ricapito, An overview of the EU breeding blanket design strategy as an integral part of the DEMO design effort, Fusion Eng. Des. 141 (2019) 30–42, http://dx.doi.org/10.1016/j.fusengdes.2019.01.141, URL https://www.sciencedirect.com/science/article/pii/S0920379619301590.

[2] R.N.S. Thomas M. Evans, K.T. Clarno, Denovo: A new three-dimensional parallel discrete ordinates code in SCALE, Nucl. Technol. 171 (2) (2010) 171–200, http://dx.doi.org/10.13182/NT171-171.

[3] M. Williams, Generalized contributon response theory, Nucl. Sci. Eng. 108 (4) (1991) 355–383, http://dx.doi.org/10.13182/NSE90-33.

[4] T. Goorley, M. James, T. Booth, F. Brown, J. Bull, L.J. Cox, J. Durkee, J. Elson, M. Fensin, R.A. Forster, J. Hendricks, H.G. Hughes, R. Johns, B. Kiedrowski, R. Martz, S. Mashnik, G. McKinney, D. Pelowitz, R. Prael, J. Sweezy, L. Waters, T. Wilcox, T. Zukaitis, Initial MCNP6 release overview, Nucl. Technol. 180 (3) (2012) 298–315, http://dx.doi.org/10.13182/NT11-135.

[5] D. Brown, M. Chadwick, R. Capote, A. Kahler, A. Trkov, M. Herman, A. Sonzogni, Y. Danon, A. Carlson, M. Dunn, D. Smith, G. Hale, G. Arbanas, R. Arcilla, C. Bates, B. Beck, B. Becker, F. Brown, R. Casperson, J. Conlin, D. Cullen, M.-A. Descalle, R. Firestone, T. Gaines, K. Guber, A. Hawari, J. Holmes, T. Johnson, T. Kawano, B. Kiedrowski, A. Koning, S. Kopecky, L. Leal, J. Lestone, C. Lubitz, J. Márquez Damián, C. Mattoon, E. McCutchan, S. Mughabghab, P. Navratil, D. Neudecker, G. Nobre, G. Noguere, M. Paris, M. Pigni, A. Plompen, B. Pritychenko, V. Pronyaev, D. Roubtsov, D. Rochman, P. Romano, P. Schillebeeckx, S. Simakov, M. Sin, I. Sirakov, B. Sleaford, V. Sobes, E. Soukhovitskii, I. Stetcu, P. Talou, I. Thompson, S. van der Marck, L. Welser-Sherrill, D. Wiarda, M. White, J. Wormald, R. Wright, M. Zerkle, G. Žerovnik, Y. Zhu, ENDF/B-VIII.0: the 8th major release of the nuclear reaction data library with CIELO-project cross sections, new standards and thermal scattering data, Nucl. Data Sheets 148 (2018) 1–142, http://dx.doi.org/10.1016/j.nds.2018.02.001, URL https://www.sciencedirect.com/science/article/pii/S0090375218300206, Special Issue on Nuclear Reaction Data.

[6] A.J.M. Plompen, O. Cabellos, C. De Saint Jean, M. Fleming, A. Algora, M. Angelone, P. Archier, E. Bauge, O. Bersillon, A. Blokhin, F. Cantargi, A. Chebboubi, C. Diez, H. Duarte, E. Dupont, J. Dyrda, B. Erasmus, L. Fiorito, U. Fischer, D. Flammini, D. Foligno, M.R. Gilbert, J.R. Granada, W. Haeck, F.-J. Hambsch, P. Helgesson, S. Hilaire, I. Hill, M. Hursin, R. Ichou, R. Jacqmin, B. Jansky, C. Jouanne, M.A. Kellett, D.H. Kim, H.I. Kim, I. Kodeli, A.J. Koning, A.Y. Konobeyev, S. Kopecky, B. Kos, A. Krása, L.C. Leal, N. Leclaire, P. Leconte, Y.O. Lee, H. Leeb, O. Litaize, M. Majerle, J.I. Márquez Damián, F. Michel-Sendis, R.W. Mills, B. Morillon, G. Noguère, M. Pecchia, S. Pelloni, P. Pereslavtsev, R.J. Perry, D. Rochman, A. Röhrmoser, P. Romain, P. Romojaro, D. Roubtsov, P. Sauvan, P. Schillebeeckx, K.H. Schmidt, O. Serot, S. Simakov, I. Sirakov, H. Sjöstrand, A. Stankovskiy, J.C. Sublet, P. Tamagno, A. Trkov, S. van der Marck, F. Álvarez-Velarde, R. Villari, T.C. Ware, K. Yokoyama, G. Žerovnik, The joint evaluated fission and fusion nuclear data library, JEFF-3.3, Eur. Phys. J. A 56 (2020) 181, http://dx.doi.org/10.1140/epja/s10050-020-00141-9.

[7] G. Schnabel, D.L. Aldama, T. Bohm, U. Fischer, S. Kunieda, A. Trkov, C. Konno, R. Capote, A.J. Koning, S. Breidokaite, T. Eade, M. Fabbri, D. Flammini, L. Isolan, I. Kodeli, M. Košťál, S. Kwon, D. Laghi, D. Leichtle, S. Nakayama, M. Ohta, L.W. Packer, Y. Qiu, S. Sato, M. Sawan, M. Schulc, G. Stankunas, M. Sumini, A. Valentine, R. Villari, A. Žohar, FENDL: A library for fusion research and applications, 2023, arXiv:2311.10063.

[8] A. Trkov, P. Griffin, S. Simakov, L. Greenwood, K. Zolotarev, R. Capote, D. Aldama, V. Chechev, C. Destouches, A. Kahler, C. Konno, M. Koštál, M. Majerle, E. Malambu, M. Ohta, V. Pronyaev, V. Radulović, S. Sato, M. Schulc, E. Šimečková, I. Vavtar, J. Wagemans, M. White, H. Yashima, IRDFF-II: A new neutron metrology library, Nucl. Data Sheets 163 (2020) 1–108, http://dx.doi.org/10.1016/j.nds.2019.12.001, URL https://www.sciencedirect.com/science/article/pii/S0090375219300687.

[9] E.M. Zsolnay, R. Capote Noy, H.J. Nolthenius, A. Trkov, Summary Description of the New International Reactor Dosimetry and Fusion File (IRDFF release 1.0), Tech. rep., International Atomic Energy Agency (IAEA) - Nuclear Data Section (NDS), 2012.

[10] D. Flammini, M. Angelone, B. Caiffi, A. Colangeli, N. Fonnesu, G. Mariano, F. Moro, R. Villari, Pre-analysis of the WCLL breeding blanket mock-up neutronics experiment at the frascati neutron generator, Fusion Eng. Des. 156 (2020) 111600, http://dx.doi.org/10.1016/j.fusengdes.2020.111600, URL https://www.sciencedirect.com/science/article/pii/S0920379620301484.

[11] I.A. Kodeli, A. Čufar, Validation of DT source term modelling in MCNP and MCUNED codes against SINBAD fusion benchmarks, Fusion Eng. Des. 154 (2020) 111542, http://dx.doi.org/10.1016/j.fusengdes.2020.111542, URL https://www.sciencedirect.com/science/article/pii/S0920379620300909.

[12] V. Radulović, R. Jaćimović, A. Pungerčič, I. Vavtar, L. Snoj, A. Trkov, Characterization of the neutron spectra in three irradiation channels of the JSI TRIGA reactor using the GRUPINT spectrum adjustment code, Nucl. Data Sheets 167 (2020) 61–75, http://dx.doi.org/10.1016/j.nds.2020.07.003, URL https://www.sciencedirect.com/science/article/pii/S0090375220300259.

[13] S.W. Mosher, S.R. Johnson, A.M. Bevill, A.M. Ibrahim, C.R. Daily, T.M. Evans, J.C. Wagner, J.O. Johnson, R.E. Grove, ADVANTG — an Automated Variance Reduction Parameter Generator, Tech. rep., Oak Ridge National Laboratory, 2013, ORNL/TM-2013/416 Rev.

[14] D. Wiarda, M. Dunn, D. Peplow, T. Miller, H. Akkurt, Development and Testing of ENDF/B-VI.8 and ENDF/B-VII.0 Coupled Neutron-Gamma Libraries for SCALE 6, Tech. rep., Oak Ridge National Laboratory, 2008, ORNL/TM-2008/047.

[15] M. Chadwick, P. Obložinský, M. Herman, N. Greene, R. McKnight, D. Smith, P. Young, R. MacFarlane, G. Hale, S. Frankle, A. Kahler, T. Kawano, R. Little, D. Madland, P. Moller, R. Mosteller, P. Page, P. Talou, H. Trellue, M. White, W. Wilson, R. Arcilla, C. Dunford, S. Mughabghab, B. Pritychenko, D. Rochman, A. Sonzogni, C. Lubitz, T. Trumbull, J. Weinman, D. Brown, D. Cullen, D. Heinrichs, D. McNabb, H. Derrien, M. Dunn, N. Larson, L. Leal, A. Carlson, R. Block, J. Briggs, E. Cheng, H. Huria, M. Zerkle, K. Kozier, A. Courcelle, V. Pronyaev, S. van der Marck, ENDF/B-VII.0: next generation evaluated nuclear data library for nuclear science and technology, Nucl. Data Sheets 107 (12) (2006) 2931–3060, http://dx.doi.org/10.1016/j.nds.2006.11.001, URL https://www.sciencedirect.com/science/article/pii/S0090375206000871, Evaluated Nuclear Data File ENDF/B-VII.0.

[16] J. Tickner, Arbitrary perturbations in Monte Carlo neutral-particle transport, Comput. Phys. Comm. 185 (6) (2014) 1628–1638, http://dx.doi.org/10.1016/j.cpc.2014.03.003, URL https://www.sciencedirect.com/science/article/pii/S0010465514000824.

[17] T. Yamamoto, H. Sakamoto, Monte Carlo perturbation calculation for geometry change in fixed source problems with the perturbation source

method, Prog. Nucl. Energy 132 (2021) 103611, http://dx.doi.org/10.1016/j.pnucene.2020.103611, URL https://www.sciencedirect.com/science/article/pii/S0149197020303565.

[18] J. Tramm, P. Romano, P. Shriwise, A. Lund, J. Doerfert, P. Steinbrecher, A. Siegel, G. Ridley, Performance portable Monte Carlo particle transport on intel, NVIDIA, and AMD gpus, 2024.

[19] S.P. Hamilton, T.M. Evans, Continuous-energy Monte Carlo neutron transport on GPUs in the shift code, Ann. Nucl. Energy 128 (2019) 236–247, http://dx.doi.org/10.1016/j.anucene.2019.01.012, URL https://www.sciencedirect.com/science/article/pii/S0306454919300167.